Conf-920673-7

DISCLAIMER

WSRC-MS--91-293

DE92 017059

MECHANICAL PROPERTIES OF 1950'S VINTAGE 304 STAINLESS STEEL WELDMENT COMPONENTS AFTER LOW TEMPERATURE NEUTRON IRRADIATION (U)

by

R. L. Sindelar, G. R. Caskey, Jr., and J. K. Thomas
Westinghouse Savannah River Company
Savannah River Site
Aiken, South Carolina 29808

J. R. Hawthorne and A. L. Hiser
Materials Engineering Associates, Inc.
9700-B Martin Luther King, Jr. Highway
Lanham, MD 20706

R. A. Lott, J. A. Begley, and R. P. Shogan
Westinghouse Electric Corporation
Science and Technology Center
Pittsburgh, PA 15235

A paper proposed for presentation at the
Effects of Radiation on Materials (16th Symposium)
Denver, CO
June 21 - 25, 1992

and for publication in the proceedings

This report was prepared in connection with work done under Contract No. DE-AC09-89SR18035 with the U.S. Department of Energy. By acceptance of this report, the publisher and/or recipient acknowledges the U.S. Government's right to retain a nonexclusive, royalty-free license in and to any copyright covering this report, along with the right to reproduce and to authorize others to reproduce all or part of the copyrighted report.

WSRC-MS-91-293

MECHANICAL PROPERTIES OF 1950'S VINTAGE TYPE 304 STAINLESS STEEL WELDMENT COMPONENTS AFTER LOW TEMPERATURE NEUTRON IRRADIATION

by

R.L. Sindelar, G.R. Caskey Jr., and J.K. Thomas
Westinghouse Savannah River Company, Savannah River Technology Center
Aiken, South Carolina 29808

J.R. Hawthorne and A.L. Hiser
Materials Engineering Associates, Inc., 9700-B Martin Luther King, Jr. Highway
Lanham, Maryland 20706

R.A. Lott, J.A. Begley, and R.P. Shogan
Westinghouse Electric Corporation, Science and Technology Center
Pittsburgh, Pennsylvania 15235

A paper proposed for presentation and publication at the Effects of Radiation on Materials (16th Symposium) in Denver, CO on June 21-25, 1992 sponsored by ASTM.

MECHANICAL PROPERTIES OF 1950'S VINTAGE TYPE 304 STAINLESS STEEL WELDMENT COMPONENTS AFTER LOW TEMPERATURE NEUTRON IRRADIATION

R.L. Sindelar, G.R. Caskey Jr., and J.K. Thomas
Westinghouse Savannah River Company, Savannah River Technology Center
Aiken, South Carolina 29808

J.R. Hawthorne and A.L. Hiser
Materials Engineering Associates, Inc., 9700-B Martin Luther King, Jr. Highway
Lanham, Maryland 20706

R.A. Lott, J.A. Begley, and R.P. Shogan
Westinghouse Electric Corporation, Science and Technology Center
Pittsburgh, Pennsylvania 15235

ABSTRACT

The reactor vessels of the nuclear production reactors at the Savannah River Site (SRS) were constructed in the 1950's from Type 304 stainless steel plates welded with Type 308 stainless steel filler using the multipass metal inert gas process. An irradiated mechanical properties database has been developed for the vessel with materials from archival primary coolant system piping irradiated at low temperatures (75 to 150°C) in the State University of New York at Buffalo reactor (UBR) and the High Flux Isotope Reactor (HFIR) to doses of 0.065 to 2.1 dpa. Fracture toughness, tensile, and Charpy-V impact properties of the weldment components (base, weld, and weld heat-affected-zone (HAZ)) have been measured at temperatures of 25°C and 125°C in the L-C and C-L orientations for materials in both the irradiated and unirradiated conditions for companion specimens. Fracture toughness and tensile properties of specimens cut from an SRS reactor vessel sidewall with doses of 0.1 and 0.5 dpa were also measured at temperatures of 25 and 125°C.

The irradiated materials exhibit hardening with loss of work hardenability and a reduction in toughness relative to the unirradiated materials. The HFIR-irradiated materials show an increase in yield strength between about 20% to 190% with a concomitant tensile strength increase between about 15% to 30%. The elastic-plastic fracture toughness parameters and Charpy-V energy absorption both decrease and show only a slight sensitivity to dose. The irradiation-induced decrease in the elastic-plastic fracture toughness (J_{def} at 1 mm crack extension) is between 20% to 65%; the range of J_{IC} values are 72.8 to 366 kJ/m^2 for the irradiated materials. Similarly, Charpy V-notch results show a 40% to 60% decrease in impact energies. The C-L orientation shows significantly lower absorbed energies and fracture toughness parameters than the L-C orientation for both the base and HAZ components in both the unirradiated and irradiated conditions.

The residual fracture toughness ($J_{1mm\ irradiated} / J_{1mm\ unirradiated}$) from the HFIR specimens are similar to those from the vessel sidewall specimens at the same dose, 0.5 dpa. The dose rate of the sidewall material (2.5 x 10^{-9} dpa/s) was approximately 100 times less than the HFIR specimens (2.6 x 10^{-7} dpa/s). Conversely, the thermal-to-fast (E_n > 0.1 MeV) fluence ratio for the vessel sidewall specimens (≈ 5) was similar to that for the HFIR specimens (≈ 3.4).

Introduction

The production reactors at the Savannah River Site (SRS) were constructed and began operation in the early 1950's. The stainless steel sidewalls of the reactor vessels have been exposed to neutron irradiation during reactor operation with nearly all of the fast fluence exposure occuring prior to 1968 when blanketed operation of the core greatly reduced the sidewall exposure rate from the pre-1968 rate. The present maximum dose to the sidewall is 1.4 dpa; the exposure occurred at sidewall temperatures < 130°C [1].

Activities for understanding irradiation effects to the reactor vessels, the development of an irradiated property database, and the application of irradiated properties to the structural integrity evaluation of the SRS reactor vessels are performed under the Reactor Materials Program (RMP) at the Savannah River Technology Center. The structural integrity evaluation of the reactor vessels includes evaluation of the impact of postulated flaws on reactor operation, as shown schematically in Figure 1. Material properties, especially fracture resistance, for low-temperature irradiated American Iron and Steel Institute (AISI) Type 304 stainless steel weldments (base, weld, and weld heat-affected-zone (HAZ)) are required inputs to flaw evaluation.

Mechanical properties were developed at testing temperatures of 25 and 125°C to span the range of vessel sidewall temperatures during reactor operation. Irradiation and testing activities were undertaken to generate site-specific irradiated properties providing a database for the fracture resistance of Type 304 and 308 stainless steels following low temperature (less than 200°C) neutron irradiation where data had been sparse. The materials, irradiations, mechanical testing details, and results are provided in this paper.

A properties database [2] was developed from the mechanical test results of Tensile (T), Charpy V-notch (CVN), Compact Tension (CT) specimens cut from SRS archival reactor piping and irradiated to 0.065 dpa in the UBR test reactor (Buffalo Materials Research Center) [3] and up to 2.1 dpa in the High Flux Isotope Reactor (HFIR) in the 4M irradiation capsule. Properties from T and CT specimens cut from sections of an SRS vessel (R-tank) sidewall with doses of 0.1 and 0.5 dpa were also measured [4, 5] and included in the database. Results from an in-reactor irradiation of T specimens of Type 304 weldments from a thermal shield model at SRS [6] and results from T, CVN, and CT specimens of Type 304L plate material irradiated up to 0.5 dpa in the HFIR 1Q capsule assembly are also discussed.

Materials

The original material of construction of the pressure boundary of the reactor primary coolant system including the reactor vessel is 1950's vintage AISI Type 304 stainless steel joined by inert-gas-shielded metal arc welding with Type 308 stainless steel filler wire. The sidewalls of the reactor vessel are constructed from plates 12.7 mm (0.5 in.) thick.

Archival primary coolant piping materials with six years of service were obtained for irradiation and mechanical testing studies [3, 7]. Specimens for the UBR and HFIR 4M irradiation were cut from eight separate sections of 12.7 mm (0.5 in.) thick piping fabricated to ASTM A-312-48T (Grade chromium-nickel). Each individual pipe section contained a circumferential butt weld and was referenced to an arbitrarily assigned pipe ring number (1 through 8). The sections were identified by a material code with the first number of this code signifying the pipe ring number. The adjacent letter indicates the material type (W = weld, B = base, and H = heat-affected-zone or HAZ); the second letter (applicable to base and HAZ material only) identifies the side with respect to the circumferential weld from which the specimen came in the pipe ring (side A or side B) as referenced in the cutting diagrams. The chemical compositions of the different base and weld metals for the eight pipe rings are given in Table 1.

The piping circumferential weld joint was a single Vee; the joint preparation contained a small land on the inner diameter (ID) side to aid preweld fitup. The joint was filled from the OD side using several weld passes following a root pass made from the ID side. Delta-ferrite measurements taken along the outer surface of the circumferential weld metal around each of the eight pipe sections show a range of 10 to 15 percent ferrite (Table 2). The measured ferrite contents are within the range of 1 to 18 percent ferrite predicted by the weld composition and the Schaeffler Diagram [8].

Four discs were cut from the sidewall of the R-reactor, a permanently shutdown reactor. The main tank shell was fabricated from five different heats of Type 304 stainless steel, two heats in the upper section and three heats in the lower section. All four discs, RA, RB, RC, and RD, were cut from the lower half of the reactor tank and came from plates 3, 4, and 5 as listed in Table 3. According to mill analyses included in the construction records, all of the steel in the tank shell was low carbon stainless steel, ≤ 0.03 weight percent, as shown in Table 3. However, recent chemical analyses of the discs yielded carbon contents of >0.05 weight percent for three of the four discs. Nickel and chromium analyses on the discs were also slightly lower than those reported in the mill analyses. Concentrations of the other constituents were consistent between the two analyses. In all cases, the analyses fall within the specifications for Type 304 stainless steel.

Specimens irradiated in the HFIR 1Q capsule assembly were machined from a wrought plate (Materials Engineering Associates Code F50) of Type 304L stainless steel. Table 4 lists the chemical composition and heat treatment of the F50 plate material.

Test specimens for the SRS irradiation program in 1959 were machined from a model of a thermal shield that had been made about the same time as the reactor tanks and thermal shields [6]. The model was constructed of 5/8-inch as-rolled plate of Type 304 stainless steel. Plates were joined by butt welding by a manual metal arc process with Type 308 electrodes with a lime coating.

The specific composition of the plates from which the thermal shield model was constructed is not available.

Table 1: Base metal chemical compositions (wt%) for archive pipe [1985 chemical analysis]

		Composition (wt-%)											
		C	Mn	Si	P	S	Ni	Cr	Mo	B	Co	Cu	N
1	A	0.079	1.60	0.79	0.031	0.011	9.36	18.79	0.41	0.001	0.11	0.29	0.047
	B	0.035	1.56	0.58	0.024	0.016	9.19	18.44	0.25	0.002	0.10	0.24	0.036
2	A	0.079	1.50	0.34	0.031	0.024	9.65	18.27	0.45	0.002	0.13	0.42	0.043
	B	0.052	1.41	0.38	0.031	0.025	8.50	19.40	0.39	<0.001	0.15	0.42	0.036
3	A	0.063	1.30	0.31	0.028	0.024	9.38	18.59	0.40	0.001	0.12	0.38	0.044
	B	0.048	1.33	0.39	0.027	0.025	9.13	18.67	0.36	0.002	0.13	0.39	0.034
4	A	0.053	1.81	0.33	0.026	0.017	8.75	18.97	0.35	0.002	0.11	0.28	0.033
	B	0.083	1.75	0.74	0.033	0.017	9.60	18.88	0.46	0.002	0.13	0.32	0.043
5	A	0.041	1.39	0.67	0.026	0.024	9.64	19.05	0.52	0.002	0.12	0.28	0.035
	B	0.080	1.25	0.32	0.026	0.016	10.0	18.88	0.44	0.001	0.13	0.41	0.043
6	A	0.058	1.44	0.49	0.027	0.017	9.65	19.05	0.43	0.001	0.15	0.62	0.044
	B	0.046	1.46	0.66	0.026	0.024	8.48	18.88	0.22	0.001	0.13	0.17	0.034
7	A	0.052	1.30	0.55	0.028	0.016	9.35	18.65	0.38	0.002	0.12	0.26	0.039
	B	0.047	1.33	0.34	0.027	0.019	9.15	18.50	0.21	0.001	0.08	0.20	0.037
8	A	0.055	1.30	0.40	0.030	0.026	8.72	19.05	0.42	0.002	0.16	0.45	0.036
	B	0.078	1.75	0.40	0.033	0.018	8.30	19.66	0.44	0.003	0.54	0.34	0.043

Table 1 (cont'd): Weld metal chemical compositions (wt%) for archive pipe

	Composition (wt-%)										
	C	**Mn**	**Si**	**P**	**S**	**Ni**	**Cr**	**Mo**	**B**	**Co**	**Cu**
1	0.038	1.39	0.41	0.023	0.018	9.65	20.15	0.23	0.002	0.11 0.11[a]	0.21 0.20[a]
2	0.052	1.45	0.41	0.022	0.019	10.50	19.20	0.20	0.005	0.10	0.22
3	0.039	1.25	0 39	0.020	0.017	10.16	19.56	0.21	0.004	0.20	0.21
4	0.047	1.41	0.43	0.022	0.018	10.75	19.29	0.17	0.005	0.094	0.20
5	0.048	1.52	0.42	0.023	0.010	10.15	19.96	0.26	0.001	0.16 0.17[a]	0.23 0.18[a]
6	0.050	1.56	0.49	0.024 0.022[a]	0.008 0.010[a]	10.12	19.87	0.24	<0.001	0.18	0.19 0.19[a]
7	0.042	1.47	0.43	0.020	0.009	9.88	19.47	0.24	0.003	0.15	0.21
8	0.045	1.52	0.37	0.022	0.018	9.70	20.15	0.21	0.002	0.22	0.18 0.16[a]

a Duplicate Analysis Using Separate Stock

Table 2: Average Ferrite Levels for Weld Material of Archive Pipe

Ring #	Weld Reference	Ferrite (%)
1	2PW216W3	13.6
2	6PW1816W3	10.0
3	4PW16W5	15.0
4	1P1W1316W3	10.7
5	2PW1716W2	11.7
6	3PW1516W5	11.2
7	4PW416W4	14.2
8	2PW216W5	14.3

Table 3: Base metal chemical compositions (wt%) for R-Tank Disks A,B,C, and D [1986 chemical analysis] and for the R-Tank plate (Nos. 1-5) composition reported by the vessel fabricator [circa 1952 analysis].

	Composition (wt-%)											
	C	Mn	Si	P	S	Ni	Cr	Mo	B	Co	Cu	N
RA	0.050	1.02	0.60	0.027	0.015	8.54	17.2	0.076	<0.005	0.05	0.121	0.009
RB	0.016	1.15	0.54	0.008	0.013	8.79	18.2	<0.01	<0.005	0.058	0.046	0.070
RC	0.054	1.24	0.57	0.017	0.022	9.28	18.2	0.35	<0.001	0.027	0.069	0.080
RD	0.077	1.26	0.55	0.020	0.022	9.73	18.7	0.34	<0.001	0.026	0.075	0.045
P* 1	0.028	0.95	0.55	0.027	0.015	9.10	18.47	NA	NA	NA	NA	NA
2	0.026	1.17	0.60	0.023	0.011	9.47	18.42	NA	NA	NA	NA	NA
3	0.023	1.20	0.63	0.015	0.024	9.12	19.00	NA	NA	NA	NA	NA
4	0.025	1.05	0.60	0.027	0.011	9.15	18.49	NA	NA	NA	NA	NA
5	0.030	1.28	0.48	0.015	0.024	9.32	18.48	NA	NA	NA	NA	NA

* Tank plates 1 and 2 were in the upper half of the tank wall and plates 3, 4, and 5 were in the lower half of the tank wall. Disks RA, RB, RC, and RD were cut from plates 3, 4, or 5; the correspondence is uncertain. Tensile and Compact Tension specimens were cut from disks RA and RD for testing at 25 and 125°C.

Table 4: Chemical composition and heat treatment of the Type 304L stainless steel material irradiated in the HFIR 1Q capsule.

	Composition (wt-%)											
	C	Mn	Si	P	S	Ni	Cr	Mo	B	Co	Cu	N
F50 Plate	0.025	1.71	0.85	0.015	0.023	10.63	19.8	0.09	NA	0.11	NA	NA

Plate thickness: 1/2 inches.
Heat Treatment: Solution annealed at 1950-2000°F for 1/2 hour, water quenched.

Test Specimens and Mechanical Testing

Mechanical properties of the base, weld, and weld heat-affected-zone (HAZ) weldment components of the archival piping were measured with T, CVN, and CT specimens in the UBR and HFIR 4M capsule irradiations. The UBR and HFIR 4M specimen tests were conducted at the Buffalo Materials Research Center. The specimens were machined in the ASTM C-L and L-C orientations to allow comparison of the mechanical response for flaws oriented parallel and perpendicular, respectively, to the pipe axis or rolling direction of the original plate.

Companion specimens, identical in material and mechanical specimen design to the irradiated specimens, were tested in the unirradiated or baseline condition [9, 10] to allow computation of the radiation-induced change in mechanical properties.

UBR and HFIR Charpy Impact and Tensile Testing

The CVN specimen dimensions conform with those of the standard size Type-A specimen identified in ASTM E 23-81, "Standard Methods for Notch Bar Impact Testing of Metallic Materials." The tensile test specimen gage dimensions (Figure 2) conform to ASTM standards E8-81 and E21-79. The specimens, test conditions, and results for the UBR specimens were previously reported in reference 3. The specimens and test conditions for the HFIR 1Q and 4M specimens are listed in Table 5.

HFIR Compact Tension Testing

Due to piping size constraints, the CT specimens were limited to a 0.4T-CT thickness, that is, a 0.394-in (10 mm) thick specimen was the maximum that could be machined from the pipe considering the curvature of the large diameter pipe stock. Design for the CT specimens was based on an evaluation of the effects of specimen size, load hole size and position, and side-grooves. All specimens were side-grooved (10% on each side or 20% total) to reduce crack tunneling and to provide an even, parallel crack front to assess crack extension. The final specimen CT design (E399 SR) [11] was used in the baseline testing [9, 10], the HFIR 1Q and 4M irradiated CT specimen tests, and for several of the R-tank CT specimen tests. The CT design is shown in Figure 3.

A conventional load cell was used to measure the applied load to the CT specimen during testing. Specimen load-line displacement was measured with an outboard clip gage. Crack extension was calibrated with single-specimen compliance techniques and rotation corrections were applied. J-integral resistance (J-R) curve analysis was performed for both the modified-J (J_M) and deformation-J (J_D) approach from the load versus crack extension data. Flow stress values, $s_f = (s_y + s_u)/2$ [where s_y and s_u are the yield (0.2% offset) and ultimate tensile strengths, respectively], were obtained from corresponding tensile data or from estimated flow stress properties in the cases where no corresponding data existed. The blunting line is given by $J = 2*(s_f)*\Delta a$. A power-law of the form $J = C(\Delta a^n)$ was fit to the data between the exclusion lines (ASTM E 813-81) with the power law toughness corresponding to the onset of stable tearing, J_{IC}, defined as the intersection of the power law curve with the 0.15 mm (0.006 in) exclusion line. Values for J_{IC} were also obtained per standard ASTM E813-81.

R-Reactor Sidewall Specimen Mechanical Testing

Base material of the R-tank was tested from the R-tank discs. Subsized T specimens and two separate CT planforms (0.4T and 0.8T) were tested in air at temperatures of 25 and 125°C [4, 5]. Specimens were held at temperature for 15-minutes before tesing. The individual specimens and test conditions for the R-tank materials are listed in Table 6. Tests at temperatures outside of the range were performed in the R-tank testing program [4, 5].

Tensile tests of the sub-sized specimens, Figure 4, were in accordance with pertinent sections of ASTM specifications E8 and E21 [12]. Initial and final specimen diameters were measured by micrometer and from 2.5X photographs, respectively. Errors in diameter measurements were ± 0.0001 and ± 0.003-inch, respectively. Specimen elongation and strain rate were calculated from cross-head travel assuming a stiff machine.

The J-integral tests for fracture toughness were all performed on compact tension specimens of the dimensions shown in Figures 3 or 5 at 25 or 125°C [4]. The four larger specimens (RA3-7A, RA3-8, RD3-7 and RD3-9) had a plan form of 0.8T-CT, but were only 0.45-inches thick. The specimen thickness and plan form were limited by the thickness and curvature of the tank wall. The four smaller specimens machined from disc RD3 were 0.394-CT specimens with 20% sidegrooves (0.315-inch thick net section). The CT specimens were tested on a 20,000 pound capacity screw driven Instron tensile machine. Crack lengths were determined by unloading compliance with load line clip gauges to measure displacements. Rotation corrections were made to the crack length measurements. Load-displacement data were collected and stored by computer for analysis by both J-deformation and J-modified procedures.

Thermal Shield Mechanical Testing

Tensile specimens cut from the base, weld, and HAZ components of a thermal shield model were 8-inches long with a gauge length of 2-inches, a width of 0.500-inches, and a thickness of 0.375-inches. Tensile tests were performed at room temperature on a 60,000 pound capacity tensile machine with a strain rate of 0.005 inch/inch/minute [6].

Table 5 HFIR 1Q and 4M Specimen Irradiation Parameters [2].

Specimen ID	Specimen Type	Orientation	Thermal Fluence, 10^{21} n/cm^2	Fast Fluence, E_n>0.1MeV, 10^{21} n/cm^2	dpa
1Q Capsule					
F50-12	T	L-T	1.2	0.36	0.21
F50-9	T	L-T	2.1	0.60	0.34
F50-1	T	L-T	2.7	0.77	0.43
F50-6	T	L-T	3.1	0.89	0.50
F50-8	T	L-T	3.2	0.92	0.52
F50-13	CVN	L-T	1.2	0.36	0.21
F50-19	CVN	L-T	2.1	0.60	0.34
F50-14	CVN	L-T	2.7	0.77	0.43
F50-23	CVN	L-T	3.1	0.89	0.50
F50-17	CT	L-T	1.2	0.36	0.21
F50-18	CT	L-T	2.0	0.58	0.33
F50-12	CT	L-T	2.3	0.67	0.38
F50-19	CT	L-T	3.0	0.88	0.50
F50-13	CT	L-T	3.1	0.90	0.51
F50-8	CT	L-T	3.2	0.92	0.52
4M Capsule					
3HA8	T	L-C	6.2	1.8	1.0
1BB1	T	L-C	9.3	2.7	1.5
5BA5	T	C-L	11.4	3.3	1.9
4BB2	T	C-L	12.8	3.7	2.1
1BB4	T	L-C	13.1	3.8	2.1
6W1	CVN	L-C	6.2	1.8	1.0
6HA6	CVN	L-C	9.3	2.7	1.5
3HB1	CVN	L-C	11.4	3.3	1.9
4BB9	CVN	C-L	12.8	3.7	2.1
1BB5	CVN	L-C	13.1	3.8	2.1
3HA5	CT	L-C	6.2	1.8	1.1
1BB8	CT	L-C	7.6	2.2	1.3
1BB16	CT	L-C	9.0	2.6	1.5
2W2	CT	L-C	10.0	2.9	1.7
5BA7	CT	C-L	11.0	3.2	1.8
3HB4	CT	L-C	11.7	3.4	1.9
7HA5	CT	C-L	12.4	3.6	2.1
7HA7	CT	C-L	12.4	3.6	2.0
1BB9	CT	L-C	12.8	3.7	2.1
4BB10	CT	C-L	13.1	3.8	2.1

Table 6 R-Tank Specimen Irradiation Parameters [2]. The temperature during irradiation was below 130°C. The R-disk A was cut at a tank azimuthal position near the peak fast fluence sector; the R-disks B & D were cut from tank azimuthal positions near the peak thermal fluence. Dpa levels are calculated from Figure 3 of reference 1.

Specimen ID	Specimen Type	Orientation	Irradiation Temp (°C)	Thermal Fluence, 10^{21} n/cm^2	Fast Fluence, E_n>0.1MeV, 10^{21} n/cm^2	dpa
RA3 Disk						
3A1c	Sub T	-	< 130	3.5	0.7	0.5
3A2a	Sub T	-	< 130	3.5	0.7	0.5
3A3c	Sub T	-	< 130	3.5	0.7	0.5
RA37	0.8T CT	-	< 130	3.5	0.7	0.5
RA38	0.8T CT	-	< 130	3.5	0.7	0.5
RD3 Disk						
4E	Sub T	-	< 130	6	0.1	0.21
4B	Sub T	-	< 130	6	0.1	0.21
5I	Sub T	-	< 130	6	0.1	0.21
3F	Sub T	-	< 130	6	0.1	0.21
RD37	0.8T CT	-	< 130	6	0.1	0.21
RD39	0.8T CT	-	< 130	6	0.1	0.21
RD314	0.4T CT	-	< 130	6	0.1	0.21
RD313	0.4T CT	-	< 130	6	0.1	0.21
RB3 Disk						
1F5	Sub T	-	< 130	6	0.1	0.21
1F3	Sub T	-	< 130	6	0.1	0.21

Irradiations

The irradiations of the archival piping materials were conducted in separate phases. The Screening Irradiation was performed in the UBR and the Full-Term Irradiation was performed in the Removable Beryllium position in the HFIR. A Surveillance Irradiation is ongoing in the K reactor at SRS [12]. The Screening Irradiation was performed in 1985 and testing of all specimens has been completed [3]. The HFIR irradiations included the 4M and 12M mechanical specimen capsules as part of the Full-Term Irradiation [13], and the 1Q qualification capsule, containing mechanical specimens of Type 304L stainless steel plate material. The testing of all specimens from the 1Q and 4M capsules has been completed with the results provided in this report. Testing of the 12M capsule has not begun.

Mechanical specimens were cut from discs removed from the R-tank sidewall at four separate tank wall locations. The R-Reactor reached initial criticality on December 28, 1953 and operated continuously from that date, with the exception of normal reactor shutdowns and shutdowns for facility improvements, until June 17, 1964, at which time reactor operations were permanently terminated.

An irradiation of tensile specimens comprised of weldment components from a thermal shield model was performed in the SRS P-Reactor in 1959. The specimens were tested at the Savannah River Laboratory in 1960 [6].

Tables 5 and 6 list the irradiation parameters for the set of specimens from the HFIR irradiations and the R-Tank. The irradiation parameters include specimen identification, weldment type and orientation, fast neutron fluence ($E_n > 0.1$ MeV), thermal neutron fluence, dpa, and irradiation temperature.

UBR Screening Irradiation

The UBR is a 2 MW light-water-cooled and moderated reactor located in the Buffalo Materials Research facility. A total of 81 CVN and 12 T specimens [3] were contained in three, independently temperature-controlled capsules designated A, B, and C, which together formed one irradiation assembly. Capsule A was placed over capsule B which itself was placed over capsule C for irradiation in the B-4 position in the fuel lattice of the UBR. To achieve fluence balancing of the specimens, capsule B, which bisects the peak neutron flux plane, was removed and replaced with a dummy capsule prior to the end of the irradiation. The experiment was loaded into the core on May 31, 1985 and the neutron exposure was completed September 6, 1985. All of the UBR specimens were irradiated to a nominal thermal and fast fluences of 1.1×10^{19} n/cm^2 and 1.1×10^{20} n/cm^2 ($E_n > 0.1$ MeV), respectively, resulting in a displacement damage level of 0.065 dpa [3].

Thermocouples welded to specimen midsections monitored temperature. The target temperature for each capsule was 120°C ± 15°C. Actual minimum and maximum thermocouple readings from twenty-two thermocouples were 113 and 132°C, respectively. Additional details of the Screening Irradiation are contained in reference 14.

HFIR Full-Term Irradiation

The HFIR is a 85 MW (100 MW prior to November 1986 extended shutdown) pressurized light water research reactor at the Oak Ridge National Laboratory. The HFIR Full-Term Irradiation was developed [13] to provide irradiated mechanical property data applicable to the SRS reactor vessel sidewall maximum conditions throughout service life. The HFIR irradiation included four separate capsules, three containing mechanical specimens and one with corrosion specimens. The 1Q mechanical capsule, the Qualification capsule (prototype for the 4M and 12M capsules) for the Savannah River irradiations, was instrumented with thermocouples, Removable Dosimeter Tubes, Backbone Dosimeter Sets, and Small Gradient Monitors to characterize the irradiation conditions in the capsules. The 1Q irradiation ran one HFIR irradiation cycle beginning June 6 and ending June 28, 1986. The 4M irradiation ran four HFIR cycles beginning July 23, 1986 to October 23, 1986.

Irradiation of the final mechanical capsule, the 12M, began July 23, 1986 and ran for twelve HFIR cycles. The 12M irradiation was completed September 17, 1991 and testing of the specimens will follow cool-down of the assembly.

Temperatures were measured at the middle and surface of the T, CVN, and CT specimens at each end of the capsule and at capsule mid-plane. The temperature ranges were 60 to 100°C for the T specimens, 80 to 140°C for the CVN specimens, and 100 to 155°C for the CT specimens.

R-Reactor Tank Irradiation

R-tank sidewalls were irradiated and temperature less than 130°C during reactor operation from 1953 to 1964. Four disks (labelled RA, RB, RC, and RD) approximately 6 inches in diameter were cut from R-tank in 1986. The disks A & C and B & D were irradiated to fast fluence (E_n > 0.1 MeV) levels of 1 and 7 x 10^{20} n/cm^2 with corresponding thermal fluences of 6 x 10^{21} and 3.5 x 10^{21} n/cm^2 [2], respectively. Table 6 contains the individual irradiation parameters of the R-tank specimens.

Thermal Shield Materials Irradiation

Twenty tensile specimens sectioned from base, weld, and heat-affected zone were irradiated in the SRS P reactor in 1959 and were tested at SRL in 1960 [6]. The maximum (calculated) irradiation temperature was 119°C. Two different nominal fast fluence levels, 2.9 x 10^{20} and 1.2 x

10^{21} n/cm^2 ($E_n > 0.1$ MeV), were achieved in the irradiation. Specimen fluences were determined by flux traverses near the specimens; uncertainty was estimated at ± 35%.

Results

The test results of each T, CVN, and CT specimen from the HFIR 1Q and 4M capsules and the T results of the R-Tank disks are listed in Tables 7 to 11. These mechanical results are plotted together with the results from the UBR [3] and Thermal Shield [6] irradiations as a function of fast fluence ($E_n > 0.1$ MeV). Figures 6A (25°C), 6B (125°C) to 8A, 8B show the tensile test results (yield and tensile strengths), Charpy V-notch results (absorbed energy), and fracture toughness results (J_D at 1 mm) for each of specimens. Figures 9A and 9B show the 25 and 125°C fracture toughness (J_D at 1 mm) data for each specimen normalized by the its respective unirradiated value. The unirradiated fracture toughnesses for the R-Tank materials in Figures 9A and 9B are taken as the average of the base component from the baseline materials testing results [9, 10].

The database involves several experimentation variables including irradiation conditions (temperature, exposure level, exposure rate, and neutron energy spectrum), weldment component (base, weld, or HAZ), orientation, material source (product form and composition), mechanical specimen configuration, and test conditions (strain rate, temperature, and testing apparatus). From the test parameters of temperature (25 and 125°C), orientation (L-C and C-L), and weldment component (base, weld, and HAZ), twelve different categories of properties are defined to differentiate factors of major importance in evaluating the mechanical response of austenitic stainless steels to low temperature neutron irradiation. Effects of irradiation temperature, exposure level, and composition are discussed separately below.

The average tensile, fracture toughness and impact mechanical properties and the change from the average unirradiated values are listed in Tables 12A (absolute value), 12B (change from unirradiated value) to 14A, 14B for the twelve categories defined by weldment component/test temperature/specimen orientation. The properties in these tables were obtained by averaging the combined set of individual irradiated property results from the UBR, HFIR 4M, and Thermal Shield irradiations. The R-tank and HFIR 1Q specimens are categorized separately. The results, representing irradiated mechanical data at exposures from 0.1 to 4 x 10^{21} n/cm^2 ($E_n > 0.1$ MeV), are averaged and categorized independent of exposure level. It is noted, however, that the irradiated results from the UBR tensile data (125°C) suggest that "saturation" in hardening for weld components tested at 125°C has not occurred at 1.1 x 10^{20} n/cm^2 ($E_n > 0.1$ MeV).

Tensile Results

The strength properties at the higher test temperature (125 °C) were slightly lower than the strength properties at the lower temperature (25 °C). Ductility as measured by either elongation or reduction in area showed little temperature dependence. No orientation effect on material tensile properties was observed for the L-C and C-L test directions.

Hardening due to irradiation is evident in all of the test data except for the tensile strength of the weld metal at 125°C. The observed decrease in tensile strength (- 6%) for the UBR irradiated 5W material (irradiated specimen 5W24) of L-C orientation was not accompanied by any unusual changes in yield strength or ductility [3]. Data from the 6W52, 7W9, and 8W7 specimens also show low (~ 65 ksi) tensile strengths; no corresponding unirradiated tests were conducted for these materials [3]. Irradiation induced changes in yield strength and ductility for the remaining weld specimens (the UBR [3] and Thermal Shield [6] weld specimens tested at 25°C) show expected results and are consistent with all data for the base and HAZ specimens.

Charpy V-Notch Results

Irradiation reduced the energy absorption under impact loading, as shown in Figure 10, for all test temperatures, orientations, and weld components. All three material types (base,weld, and HAZ) show a slight temperature dependence with lower impact energies at the lower temperature, an effect reported earlier for irradiated Type 304L and 347 stainless steels [15]. Irradiation effects in the base and HAZ specimens were more pronounced at 125°C than at 25°C.

The average energy absorption (Table 14A) exceeded 50 ft-lbs for base metal, weld metal and HAZ material at both 25 and 125°C. These impact test results show a high toughness of Type 304 stainless steel for the temperature range of operation, all three material types (base, weld, and HAZ), and both ASTM specimen orientations. The lowest impact energies were for the C-L orientation at both test temperatures. These observations suggest that segregation, ferrite stringers, or texture effects associated with plate forming operations are particularly sensitive to irradiation. Comparison of the UBR and 4M data indicates no statistically significant decrease in impact energies with increased fast fluence ($E_n > 0.1$ MeV) from 1.1×10^{20} n/cm^2 to 3.8×10^{21} n/cm^2.

Compact Tension Results

The $J_{deformation}$-R curves for the 0.4T planform HFIR 4M specimens are shown in Figures 11 to 20. Average fracture toughness properties for the three weldments (base, weld and HAZ) are given in Table 14A. Reductions in fracture toughness due to irradiation (Table 14B) depended on both the weldment component and the specimen orientation. The largest reductions in toughness occurred for the HAZ specimens and the smallest for the base metal. The C-L orientation, where the crack runs parallel to any stringers or segregation in the steel, was especially sensitive to irradiation, an effect seen also in the CVN absorbed impact energy for both the base and HAZ weldment components. This strong dependency of the toughness on orientation was also observed in the baseline testing of these materials [9, 10]

The R-Tank materials were tested with both a small (0.4T) planform design and a large (0.8T) design. The fracture toughness results at 125°C (Table 14A) show the 0.4T to have a lower toughness than the 0.8T results. The difference is attributed to the effect of the 20% sidegrooves in the 0.4T design whereas the 0.8T specimens were not sidegrooved. A study of the effect of sidegrooving was conducted during the design of the 0.4T specimens [11]. With sidegrooving, both the 0.4 and 0.8T planforms have similar J-R curves up to crack extensions of 3 mm [9, 11].

The unirradiated CT testing results from the baseline specimens [9, 10, 11] show that no significant dependency on temperature at temperatures between 25 and 125°C. It is assumed that the irradiated specimens would exhibit a similar insensitivity to temperature at this range.

Fracture surfaces of several CVN and T specimens were examined by scanning electron microscopy (SEM) [5, 11]. Materials selected for examination included: base, weld, and heat-affected-zone (HAZ); CVN specimens irradiated in UBR and tested at 25 and 125°C; and a base metal T specimen from R-tank wall tested at 25°C. All CVN test specimens and all three material types exhibited ductile fracture at both test temperatures [11]. The tensile specimens machined from the R-tank discs A and D failed by ductile fracture at both 25 and 125°C. SEM analysis of the fracture surface of the specimens tested at 25°C showed microvoid coalescence [5].

Table 7 **Tensile Test Results at for Type 304L (F50) and Type 304 Stainless Steel (Archival Materials) Unirradiated and Irradiated Tests at 125°C [11].**

Specimen Number	Test Temp. (°C)	Yield (MPa)	Strength (ksi)	Tensile (MPa)	Stength (ksi)
		UNIRRADIATED CONDITION			
F50-115	24	288	41.74	619	---------
F50-117	24	253	36.74	612	88.75
F50-113	125	208	30.11	480	69.62
F50-101	125	193	28.01	475	68.82
F50-86	125	190	27.59	475	68.95
F50-108	125	205	29.68	470	68.13
		IRRADIATED, HFIR ASSEMBLY 1Q			
F50-1	125	462	67.05	563	81.70
F50-6	125	445	64.46	527	76.44
F50-8	125	435	63.14	513	74.34
F50-9	125	471	68.26	570	82.68
F50-12	125	448	64.94	559	81.01

Archival Materials (4M)

	Yield (MPa)	Strength (ksi)	Tensile (MPa)	Stength (ksi)
1BB1	----	71.2	----	84.4
1BB4	----	74.6	----	85.6
4BB2	----	76.7	----	88.8
5BA5	----	72.2	----	83.9
3HA8	----	81.2	----	88.6

Postirradiation Tensile Ductility of HFIR Assembly 1Q and 4M Specimens[a]

Assembly	Specimen No.	Reduction of Area (%)	Elongation in 20.3 mm (%)	Fracture Appearance
HFIR 1Q	F50-1	73.5	36.6	Cup/cone
	F50-6	66.2[b]	33.0[b]	Prongs/slant fracture
	F50-8	40.7	19.8[c]	Cup/cone
	F50-9	72.4	41.0	Prongs
	F50-12	51.0	37.8[c]	Slant fracture
HFIR 4M	1BBH1	64.6	62.2c	Slant Fracture
	1BBH4	72.4	43.0	Slant Fracture
	4BBH2	71.4	42.4	Prongs
	5BAH5	75.5	32.0	Cup/cone
	3HAH8	-[d]	-[d]	-

[a] 5.08-mm (o.200-in.) gage diameter specimens tested at 125°C

[b] Measurements questioned (Specimen halves failed to mate readily)

[c] Elongation in 13.4-mm referenced by extensometer knife edge marks (20.3-mm reference marks lost)

[d] Specimen fractured at gage marks.

Table 8 R-Tank Sub-Size Tensile Results at 25 and 125°C [5]. The cross-head speed was 0.01 inches per minute for all specimens except 3F which was tested at 0.002 inches per minute.

Spec. Location	Spec. No.	Test Temp. °F	Helium (appm)	UTS-xksi	YS-ksi	Unif. %E	Tot. %E	%RA
RA3								
ID	3A1c	75	33.5	106.9	83.2	50.4	62.5	77.5
Midwall	3A2a	75	33.7	106.4	78.8	53.3	64.2	68.4
OD	3A3c	75	33.9	97.7	62.5	40.2	52.2	76.0
RD3								
Midwall	4E	257	12.5	87.8	67.3	25.5	30.0	66.2
Midwall	4B	257	12.5	94.9	66.1	44.8	54.0	73.0
OD	5I	75	5.9	107.9	76.2	35.5	45.2	57.0
OD	3F	257	5.9	88.3	59.6	31.9	42.4	55.8
RB3								
ID	1F5	75	12.0	103.5	71.2	32.4	43.4	57.5
OD	1F3	75	3.25	106.8	76.8	32.9	46.0	75.6

Table 9 Charpy V-Notch Test Results for Type 304L (f50) and Type 304 Stainless Steel (Archival) Unirradiated and Irradiated Tests at 125°C [11].

Specimen No.	Orientation	Energy Absorption (J)	(ft-lb.)	Lateral (mm)	Expansion (mils)
		UNIRRADIATED			
88	LT	220	162	2.210	87
90	LT	247	182	2.108	83
93	LT	244	180	2.210	87
92*	LT	199	147	2.032	80
		IRRADIATED, HFIR CAPSULE ASSEMBLY 1Q			
13	LT	117	85	2.261	89
14	LT	107	79	1.702	67
19	LT	118	87	2.032	80
23	LT	108	80	2.057	81

* 24°C test temperature

Charpy V-Notch Test Results for Piping Materials (HFIR Assembly 4M; 125°C Tests)

Specimen No.	Orientation	Energy Absorption (J)	(ft-lb.)	Lateral (mm)	Expansion (mils)
4BBH9	C-L	87	64	1.397	55
1BBH5	L-C	134	99	2.007	79
3HBH1	L-C	102	75	1.397	55
6HAH6	L-C	110	81	1.600	63
6WH1	L-C	114	84	1.727	68

Table 10 Deformation J Analysis for Type 304L Stainless Steel Plate (F50) Unirradiated and HFIR 1Q Irradiated Tests at 125°C (0.394T-CT, 20% SG)

Specimen Number	ASTM E 399[a] Orientation	$(a/W)_i$	Δa_m (mm)	$\Delta a_p - \Delta a_m$ (mm)	J_{Ic} Power Law (kJ/m^2)	J_{Ic} ASTM (kJ/m^2)	T_{avg} Power Law	T_{avg} ASTM	Flow Stress (MPa)	J=8.8T (kJ/m^2)	E 813[b] Validity	Exponent N	Coefficient C (kJ/m^2)
Unirradiated													
F50-76	L-T	0.539	3.66	-0.43	428.0	435.5	244	227	336.9	(>722.9)	IV	0.3890	469.5
F50-77	L-T	0.529	3.51	-0.48	437.8	435.2	240	245	336.9	(>714.9)	IV	0.3804	476.0
Irradiated, HFIR Capsule Assembly 1Q													
F50-8	L-T	0.554	5.08	-0.59	243.3	250.9	100	99	473.9	463.9	IV	0.3572	334.8
F50-12	L-T	0.546	5.94	-0.93	266.2	266.7	85	83	516.6	466.2	IV	0.3342	358.5
F50-13	L-T	0.547	5.59	-0.92	274.6	276.6	114	119	473.9	476.0	IV	0.3747	372.8
F50-17	L-T	0.527	5.57	-1.53	294.2	302.7	109	105	503.1	504.6	IV	0.3783	399.7
F50-18	L-T	0.546	5.53	-1.08	260.0	266.0	109	105	520.3	530.2	IV	0.4147	379.3
F50-19	L-T	0.531	6.00	-0.95	251.2	261.9	129	124	485.7	506.1	IV	0.4390	371.1

[a] Specimen designation
[b] IV = ASTM invalid (specimen thickness insufficient)

Table 11 Deformation J Analysis for Type 304 Stainless Steel (Archival Materials) Unirradiated and HFIR 4M Irradiated Tests at 125°C (0.394-CT, 20% SG). Results of Additional Unirradiated Tests are Reported in References 9 and 10.

Specimen Number	ASTM E 399[a] Orientation	$(a/W)_i$	Δa_m (mm)	$\Delta a_p - \Delta a_m$ (mm)	J_{Ic} Power Law (kJ/m^2)	J_{Ic} ASTM (kJ/m^2)	T_{avg} Power Law	T_{avg} ASTM	Flow Stress (MPa)	J=8.8T (kJ/m^2)	E 813[b] Validity	Exponent N	Coefficient C (kJ/m^2)
						Unirradiated							
1BB-40	L-C	0.532	5.39	-0.82	562.7	555.0	293	288	314.7	855.6	IV	0.3850	552.8
1BB-41	L-C	0.515	6.06	-0.92	681.4	678.8	227	223	314.7	913.7	IV	0.2886	641.0
1BB-42	L-C	0.547	4.77	-0.73	650.5	643.4	267	265	314.7	857.0	IV	0.3390	613.8
4BB-113	C-L	0.532	5.49	-0.89	354.0	344.6	218	225	342.8	607.4	IV	0.3866	413.5
5BA-41	C-L	0.516	5.26	-0.28	221.7	208.5	244	258	324.2	545.9	IV	0.4701	308.7
2W-164	L-C	0.521	4.96	-0.61	339.6	335.1	225	227	415.7	690.0	IV	0.5015	453.7
2W-132	L-C	0.512	5.86	-0.73	320.0	305.1	273	275	415.7	801.5	IV	0.5879	460.9
7HA-3	L-C	0.552	5.25	-0.70	662.7	678.6	199	178	399.40	919.9	IV	0.3454	666.7
7HA-4	L-C	0.570	5.59	-0.82	617.9	605.9	200	204	399.40	879.9	IV	0.3548	634.9
4HA-61	L-C	0.542	5.87	-0.87	460.4	459.5	171	167	399.40	702.6	IV	0.3443	513.3
4HA-64	L-C	0.548	5.36	-0.80	404.6	419.5	188	170	399.40	707.3	IV	0.3904	476.0
7HA-12	C-L	0.537	4.99	-0.66	153.2	150.2	121	126	399.40	387.6	IV	0.4122	237.7
						Irradiated, HFIR Capsule Assembly 4M							
1BBH-8	L-C	0.538	6.06	-0.88	327.6	327.5	122	125	544.1	689.6	IV	0.4310	460.6
1BBH-9	L-C	0.519	6.47	-1.06	248.2	247.0	138	141	544.1	587.2	IV	0.5255	412.3
1BBH-16	L-C	0.517	6.07	-0.79	334.4	341.1	120	115	544.1	660.3	IV	0.4223	464.2
4BBH-10	C-L	0.519	6.33	-1.01	194.0	192.8	53	55	570.6	332.9	IV	0.3059	274.2
5BAH-7	C-L	0.524	5.89	-0.90	135.7	113.2	86	106	538.3	352.3	IV	0.4847	252.2
2WH-2	L-C	0.512	5.42	-0.48	140.7	135.8	77	80	599.8	385.8	V	0.4979	270.1
3HAH-5	L-C	0.536	5.84	-0.74	186.6	175.2	76	87	585.1	403.8	V	0.4229	305.4
3HBH-4	L-C	0.527	5.62	-0.71	156.6	150.1	75	88	585.1	338.6	V	0.4550	276.6
7HAH-5	C-L	0.538	6.40	-0.99	77.8	88.3	11	7	585.1	96.0	IV	0.1600	99.1
7HAH-7	C-L	0.514	5.80	-0.53	72.8	77.2	25	24	585.1	137.8	V	0.3162	118.4

[a] Specimen designation
[b] IV = ASTM invalid (specimen thickness insufficient)
[c] Estimated Value

Table 12A: As-Irradiated Tensile Data [2]

Material	Test Temperature (°C)	Sample ASTM Orientation	Engineering Yield (0.2%) Strength (ksi)	Engineering Tensile Strength (ksi)	Total Elongation* (%)	Reduction in Area (%)
Base	[illegible]	L-C	87.4	102.5	34.5	NR
		C-L	86.2	101.7	41.5	NR
R-Tank		-	74.8	104.9	52.3	68.7
Base	125	L-C	72.9	85.0	52.6	68.5
		C-L	74.5	86.4	37.2	73.5
R-Tank		-	64.3	90.3	42.1	65.0
Type 304L		L-T	65.6	79.2	33.6	60.8
HAZ	25	L-C	88.4	102.5	32.0	NR
		C-L	89.5	103.1	40.5	NR
HAZ	125	L-C	81.2	88.6	NR	NR
		C-L	-	-	-	-
Weld	25	L-C	90.1	104.2	36.5	60.8
		C-L	96.0	105.5	27.4	52.7
Weld	125	L-C	55.9	64.6	36.0	72.6
		C-L	60.2	65.2	32.0	59.3

Notes: 1) The results for the **Base, HAZ**, and **Weld**, L-C and C-L orientations are comprised of the average of the properties from the UBR [3], HFIR 4M and Thermal Shield [6] individual specimens.
2) The number of mechanical specimens in the various test categories are listed in parentheses in the average yield strength column.
3) Specimens from a plate of Type 304L SS were irradiated in the HFIR 1Q capsule.
4) The range of the Modulus of Elasticity (Young's Modulus) for the Thermal Shield specimens is 24.4×10^6 to 30.4×10^6 psi. The range of Young's Modulus for the HFIR 4M specimens is 27.3×10^6 to 36.1×10^6 psi [2].

*: Total Elongation in respective gage lengths
NR = Not Reported

Table 12B: As-Irradiated Tensile Data (Average Change from Unirradiated Strengths) [2]

Material	Test Temperature (°C)	Sample ASTM Orientation	ΔYield Strength (ksi)	ΔTensile Strength (ksi)	Yield: ΔIrr/Unirr (%)	Tensile: ΔIrr/Unirr (%)
Base	25	L-C	53.3	19.3	156	23
		C-L	52.1	18.2	153	22
R-Tank		-	36.3*	12.9*	97*	14*
Base	125	L-C	47.5	19.2	187	29
		C-L	44.3	18.2	147	27
R-Tank		-	35.3*	19.3*	122*	27*
Type 304L		L-T	36.8	10.4	128	15
HAZ	25	L-C	49.3	18.4	126	22
		C-L	50.4	19.3	129	23
HAZ	125	L-C	-	-	-	-
		C-L	-	-	-	-
Weld	25	L-C	40.0	15.6	80	18
		C-L	38.5	17.4	67	20
Weld	125	L-C	10.0	-6.2	22	-9
		C-L	-	-	-	-

*Unirradiated values for R-Tank assumed equivalent to the average (L-C & C-L) baseline properties at 25 and 125°C (9, 10)

Table 13A: As-Irradiated Charpy Impact Data [2]

Material	Test Temperature (°C)	Sample ASTM Orientation	Energy Absorption (ft-lbs)	Lateral Expansion (mils)
Base	25	L-C	83	67
		C-L	63	50
Base	125	L-C	94	80
		C-L	71	66
Type 304L	125	L-T	83	79
HAZ	25	L-C	80	59
		C-L	54	43
HAZ	125	L-C	84	66
		C-L	63	56
Weld	25	L-C	64	50
		C-L	-	-
Weld	125	L-C	87	77
		C-L	78	65

The results for the **Base, HAZ,** and **Weld**, L-C and C-L orientations are comprised of the average of the properties of the UBR and HFIR 4M data. Specimens from a plate of Type 304L SS were irradiated in the HFIR 1Q capsule.

Table 13B: As-Irradiated Charpy Impact Data (Average Change from Unirradiated Impact Energy) [2]

Material	Test Temperature (°C)	Sample ASTM Orientation	Energy Absorption (Decrease) Δft-lbs; ΔIrr/Unirr (%)	Lateral Exp. (Decrease) Δmils; ΔIrr/Unir(%)
Base	25	L-C	66; 44	13; 16
		C-L	53; 46	43; 52
Base	125	L-C	135; 59	7; 8
		C-L	57; 44	11; 14
Type 304L		L-T	92; 53	7; 8
HAZ	25	L-C	56; 41	21; 26
		C-L	41; 43	30; 41
HAZ	125	L-C	104; 55	19; 22
		C-L	38; 38	25; 31
Weld	25	L-C	49; 43	34; 40
		C-L	-	-
Weld	125	L-C	87; 50	2; 2
		C-L	97; 55	18; 22

Table 14A: As-Irradiated Fracture Toughness Data (Deformation-J, Power law fit) [2]

Material	Test Temperature (°C)	Sample ASTM Orientation	J_{IC} - Deformation (in-lb/in^2)	J @ Δa = 1mm (in-lb/in^2)	Ave Tearing Modulus
Base	25	L-C	-	-	-
		C-L	-	-	-
R-Tank		-	2092 (0.8T)	2900	125
Base	125	L-C	1730	2547	127
		C-L	942	1502	70
R-Tank		-	1730 (0.8T)	2500	125
		-	1122 (0.4T)	1800	95
Type304L		LT	1513	2107	108
HAZ	25	L-C	-	-	-
		C-L	-	-	-
HAZ	125	L-C	982	1662	76
		C-L	428	662	18
Weld	25	L-C	-	-	-
		C-L	-	-	-
Weld	125	L-C	805	1542	77
		C-L	-	-	-

*R-Tank 25°C data from 0.8T planform specimens; R-Tank 125°C data from 0.4 and 0.8T planform specimens

The results for the **Base**, **HAZ**, and **Weld**, L-C and C-L orientations are comprised of the average of the properties of the HFIR 4M data. Specimens from a plate of Type 304L SS were irradiated in the HFIR 1Q capsule.

Table 14B: As-Irradiated Fracture Toughness Data (Deformation-J, Power law fit) (Average Change from Unirradiated Values) [2]

Material	Test Temperature (°C)	Sample ASTM Orientation	J @ 1mm Irr/Unirr (Ratio;%Δ)	Ave Tearing Modulus Irr/Unirr (Ratio;%Δ)
Base	25	L-C	-	-
		C-L	-	-
R-Tank*		-	(0.8T) 0.83; -17%	0.62; -38%
Base	125	L-C	0.74; -26%	0.48; -52%
		C-L	0.73; -27%	0.30; -70%
R-Tank*		-	(0.8T) 0.90; -10%	0.53; -47%
		-	(0.4T) 0.65; -35%	0.40; -60%
Type304L		L-T	0.78; -22%	0.45; -55%
HAZ	25	L-C	-	-
		C-L	-	-
HAZ	125	L-C	0.50; -50%	0.40; -60%
		C-L	0.35; -65%	0.12; -88%
Weld	25	L-C	-	-
		C-L	-	-
Weld	125	L-C	0.59; -41%	0.31; -69%
		C-L	-	-

*Unirradiated values for R-Tank assumed equivalent to the average (L-C & C-L) baseline properties at 25 and 125°C (from reference 35)

Discussion

The specimens in the database were irradiated at temperatures from 75 to 150°C. A comprehensive study of the effect of irradiation temperature on the room temperature tensile properties of Type 304 stainless steel had been conducted by Bloom, et al [16]. The results of that study show that the mechanical properties would be insensitive to temperature at the irradiation conditions for the database. The irradiation was conducted in the B-8 position of the Oak Ridge Research Reactor and the specimens were irradiated to thermal and fast fluences of 9 x 10^{20} n/cm^2 and 7 x 10^{20} n/cm^2 (E_n > 1 MeV), respectively. [In the ORR experiment position A-9, adjacent to the B-8 position, the fast fluence ($E_n > 0.1$ MeV) is approximately 2.5 times the fast fluence ($E_n > 1$ MeV), [21]]. The irradiation temperatures in the Bloom experiments [16], 93 to 454°C, span the temperatures of the specimens in the present study. The results show that irradiation at 93 to 300°C produced a high density of defect clusters on the order of 10 nm diameter and that the yield and ultimate strengths were of approximately 90 to 100 and 115 ksi, respectively. Characterization of the microstructure of the R-Tank RA disk [17] was recently performed and also showed the dominant feature to be produced during irradiation is a high density (10^{17} cm^{-3}) of defect clusters of non-specific geometry with a most-probable size of approximately 2 nm.

Effects of fast fluence on the tensile properties of Type 304, 316 and 347 stainless steels for a low temperature (< 100°C) irradiation in the High Flux Reactor at Petten, the Netherlands were reported by Higgy and Hammad [18]. Yield points in the stress-strain curves for the stainless steels were observed at fluences of 1.3×10^{19} n/cm^2 ($E_n > 1$ MeV) and above. A saturation of radiation hardening (increase in yield strength) at a fast fluence level of 4×10^{19} n/cm^2 ($E_n > 1$ MeV) (see Figure 5-5B) was reported. A correlation was developed showing the change in yield strength to be linear with the square root of fast fluence from the minimum investigated fluence of 1.15×10^{18} n/cm^2 ($E_n > 1$ MeV) to the saturation fluence.

Although the change (from initial or unirradiated) in the tensile properties of austenitic stainless steels with fluence appears constant above a "saturation" fluence level, "saturation" of the irradiated properties or a saturation exposure level are not rigorously defined in the literature. A trend of a slight increase in radiation hardening (yield strength) or change in other mechanical properties may occur at fluences above the "saturation fluence." Note that plotting mechanical property data on a graph that is linear in fluence may appear to "show" a saturation in properties whereas a plot on a log scale shows a slight change in properties, especially when the data spans one or more decades of exposure.

Several of the data in the as-irradiated database are of the same material (e.g. 1BB material), allowing an assessment of saturation in changes in mechanical properties. The tensile results from the Thermal Shield irradiation to fast fluence levels of 2.9×10^{20} and 1.2×10^{21} n/cm^2 (En > 0.1 MeV) (see Figure 6A) indicate that saturation in the ultimate tensile and yield strengths of base, weld, and HAZ components (each of common material heat) occurs by a fluence level of approximately 2.9×10^{20} n/cm^2 ($E_n > 0.1$ MeV). Similarly, the R-tank T specimens irradiated to 1 and 7×10^{20} n/cm^2 ($E_n > 0.1$ MeV) also show no strong dependency of hardening with fluence at this exposure range although there is significant scatter in the yield strength data (see Figure 6A).

The 1Q material (F50 code Type 304L stainless steel) irradiated to fast fluence levels from 3.6 to 9.2×10^{20} n/cm^2 ($E_n > 0.1$ MeV) has similar strength values (from T specimens) and toughness values (from CVN and CT specimens) (see Figures 6B to 8B). Also the data from the 4M CT specimens of 1BB material irradiated to fast fluences of 2.2, 2.6, and 3.7×10^{21} n/cm^2 (E_n

> 0.1 MeV) with fracture toughess values (J_{def} @ 1mm) of 2621, 2641, and 2346 in-lb/in^2, respectively, do not show any significant decrease with fluence. The toughness data (J_{def} @ 1mm) from R-tank specimens RD37 and RD39 at 1 x 10^{20} n/cm^2 (tested at 125°C) are 2700 and 2500 in-lb/in^2, similar to the values from RA37 and RA38 at 7 x 10^{20} n/cm^2 (tested at 25°C), 2900 in-lb/in^2 for both. Thus, the change in toughness with fluence for a similar weldment component (and heat of material) is not significant at the exposure levels of the as-irradiated database.

The CT test results (see Figures 8A,B and 9A,B) from the R-Tank materials can be compared to the HFIR-irradiated materials to evaluate potential differences in toughness levels due to differences in irradiation conditions, specifically exposure rate and neutron spectra. Due to the small sensitivity of the mechanical response (for a common material, ie, weldment component and material heat) to fluence at the irradiation conditions of the austenitic stainless steel materials in the database, spectral and exposure rate differences would not be expected to have a significant impact. To confirm this assumption, a common heat (melt) of material should be irradiated for the irradiation conditions of interest. However, if several different material heats are involved, as is the case for the database in this study, normalization of the irradiated test response to the unirradiated response allows the impact of irradiation variables to be examined. The results for the 1Q specimens (125°C) can be compared to the R-Tank specimens (25°C) at the same fluence of 7 x 10^{20} n/cm^2 (0.5 dpa). The dose rate of the sidewall material (2.5 x 10^{-9} dpa/s) was approximately 100 times less than that for the HFIR specimens (2.6 x 10^{-7} dpa/s). The thermal-to-fast (E_n > 0.1 MeV) fluence ratio was approximately 5 for the vessel sidewall specimens at 0.5 dpa and 3.4 for all the HFIR specimens. The residual fracture toughness ($J_{1mm\ irradiated} / J_{1mm\ unirradiated}$) of approximately 80% is similar for the HFIR specimens and the vessel sidewall specimens. Thus, the test data support that, within the range examined, dose rate and spectrum do not significantly influence the irradiated property values.

The results of residual toughness (see Figure 9B and Table 5) indicate that the HAZ is the weldment component most sensitive to irradiation. Microstructurally, the HAZ component differs from the base component in that the HAZ contains chromium carbide precipitates at the grain boundaries. Characterization of the grain boundary microstructures and microchemistries of the irradiated and unirradiated materials will be performed in future work to further address the differences in fracture response of the weldment components.

Application of Irradiated Properties to SRS Vessel Structural and Fracture Analyses

The irradiated properties results were produced at fast fluences bounding reactor tank wall fluences and are input to the structural analyses (Figure 1). The application of initial design values for Types 304 plate materials and Type 308 weld material properties remain valid in the stress analyses of the reactor vessels under normal operating temperature conditions; these analyses are not affected by the increase in the yield and tensile strengths for loading conditions below design yield. For loading conditions resulting in stress levels above design yield, but below the irradiated yield strengths, the tank sidewalls would not undergo plastic deformation.

Nuclear construction or inspection codes do not specify material properties for irradiated austenitic stainless steel weldment components in either design or flaw evalution criteria. Material fracture toughness parameters for elastic-plastic fracture mechanics analysis of postulated flaws in the SRS vessels have been developed from the SRS properties database. The fracture mechanics methodology applied to the vessels involves the J-T criterion to establish flaw stability. For this methodology, the material J-T curve is readily constructed from the J-R curve, as shown below:

$$J = C\Delta a^{N}$$

with,

$$T = \left(\frac{(C)\,(N)}{\Delta a^{N-1}}\right)\left(\frac{E}{s_f^{2}}\right)$$

where the expression for J is the power law formulation of the J-R curve data with the coefficient parameter, C, and the exponent parameter, N and T is the tearing modulus. Crack extension (Δa) to 3 mm has been applied in the calculation of stable flaw sizes for the SRS vessels. Additional details of the application of the irradiated properties in the fracture assessment of the vessels is provided in references 1, 2, 19, and 20.

Conclusions

A property database of mechanical properties for Type 304 stainless steel weldment components following low temperature (< 150°C) neutron irradiation has been developed for evaluation of irradiation effects and input into vessel structural and fracture analyses at exposures up to 3.8×10^{21} n/cm^2 ($E_n > 0.1$ MeV) or 2.1 dpa. Changes in yield and tensile strengths show radiation hardening with a marked loss in work-hardenability but with high (> 15%) ductility for all components at the testing temperatures of 25 and 125°C. High toughness exceeding 40% residual ($J_{1mm\ irradiated} / J_{1mm\ unirradiated}$) is also maintained for base, weld, and HAZ components. Flaw-specific analyses should consider flaw orientation in the material due to a strong dependency of material toughness on orientation.

References

1. Sindelar, R.L., Awadalla, N.G., Baumann, N.P, and Mehta, H.S., **"Life Extension Approach to the Reactor Vessel of a Nuclear Production Reactor,"** in *Life Assessment and Life Extension of Power Plant Components*, PVP-Vol. 171, American Society of Mechanical Engineers, 1989.

2. Sindelar, R.L. and Caskey, G.R., **"Reactor Materials Program - Mechanical Properties of Irradiated Types 304 and 304L Stainless Steel Weldment Components (U),"** Westinghouse Savannah River Co. report *WSRC-TR-91-11*, Savannah River Laboratory, December 1991.

3. Hawthorne, J.R., Menke, B.H., Awadalla, N.G., and O'Kula, K.R., **"Experimental Assessments of Notch Ductility and Tensile Strength of Stainless Steel Weldments After 120°C Neutron Irradiation,"** *Influence of Radiation on Material Properties: 13th International Symposium (Part II), ASTM STP 956*, F.A. Garner, C.H. Henager, Jr., and N. Igata, Eds., American Society for Testing and Materials, Philadelphia, 1987, pp. 191-206.

4. Lott, R.G. and Begley, J.A., **"SRP Reactor Operability Assurance Program: Fracture Toughness of Savannah River R-Tank Material,"** Westinghouse Electric Corporation, Research and Development Center report *WSRP-004*, April 1987.

5. Cunningham, J.W., Shogan, R.P., Jacko, R.J., and Wood, S., **"SRP Reactor Operability Assurance Program: Tensile Properties of Savannah River Materials,"** Westinghouse Electric Corporation, Research and Development Center report*WSRP-005*, March 1987.

6. Joseph, J.W. Jr., **"Mechanical Properties of Irradiated Welds in Stainless Steel,"** E.I. du Pont, de Nemours. & Co. report *DP-534*, Savannah River Laboratory, December 1960.

7. Stoner, K.J., **"Reactor Materials Program - Materials Source History for Type 304 Stainless Steel Testing Program,"** E.I. du Pont, de Nemours, & Co. report *DPST-88-1010*, Savannah River Laboratory, December 1988.

8. Nipples, E.F., Metals Handbook, Ninth Edition, Volume 6 - Welding, Brazing, and Soldering, American Society for Metals, 1982.

9. Stoner, K.J., Sindelar, R.L., and Caskey, G.R., **"Reactor Materials Program - Baseline Material Property Handbook-Mechanical Properties of 1950's Vintage Stainless Steel Weldment Components (U),"** Westinghouse Savannah River Co. report *WSRC-TR-91-10*, Savannah River Laboratory, April 1991.

10. Stoner, K.J., Sindelar, R.L., Awadalla, N.G., Hawthorne, J.R., Hiser, A.L., and Cullen, W.H., **"Mechanical Properties of 1950's Vintage Type 304 Stainless Steel Weldment Components"**, in *Fatigue, Degradation, and Fracture* PVP-Vol. 195, American Society of Mechanical Engineers, 1990.

11. Hawthorne, J.R., et. al., **"Sample Preparation, Irradiation, and Testing of 304 Stainless Steel Specimens,"** Materials Engineering Associates, Materials Engineering Associates report *MEA-2221*, August 1987; Hawthorne, J.R. et.al., **"Parametric Study**

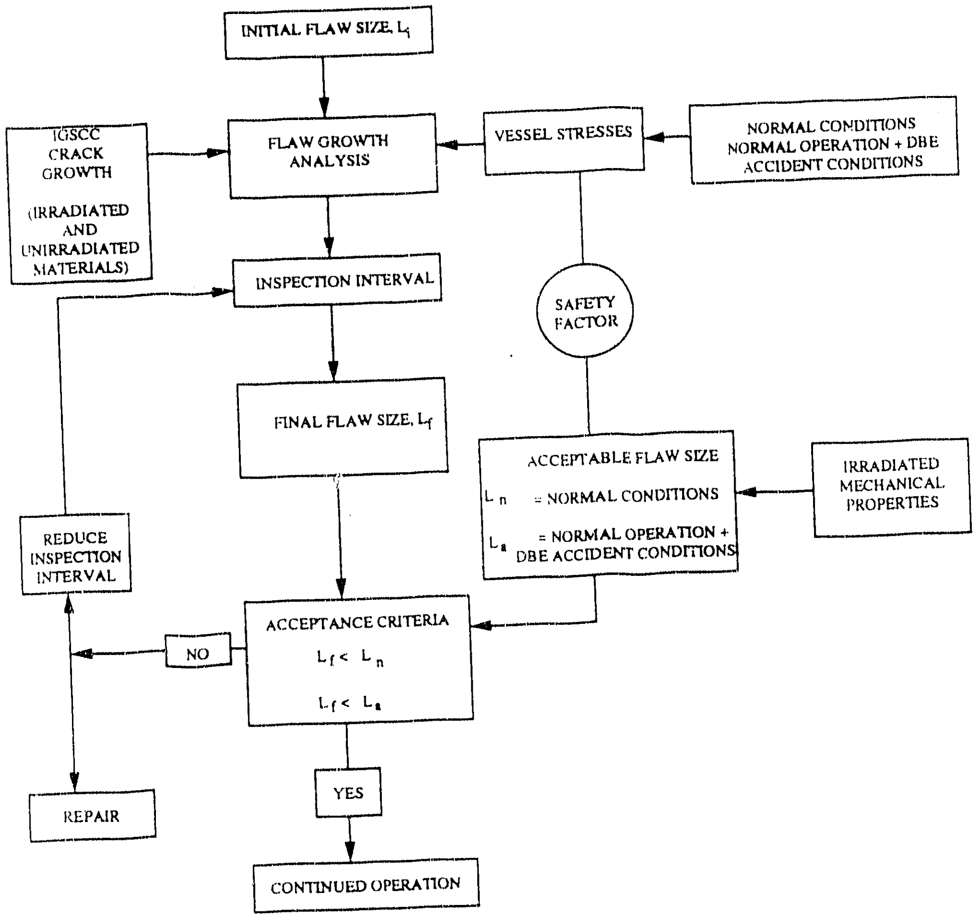

Figure 1: Schematic of the SRS Vessel Flaw Evaluation Sequence

Type	DIM "A"	DIM "B"
1	7/16 - 14 UNC	0.340 TYP
2	5/16 - 18 UNF	0.235 TYP

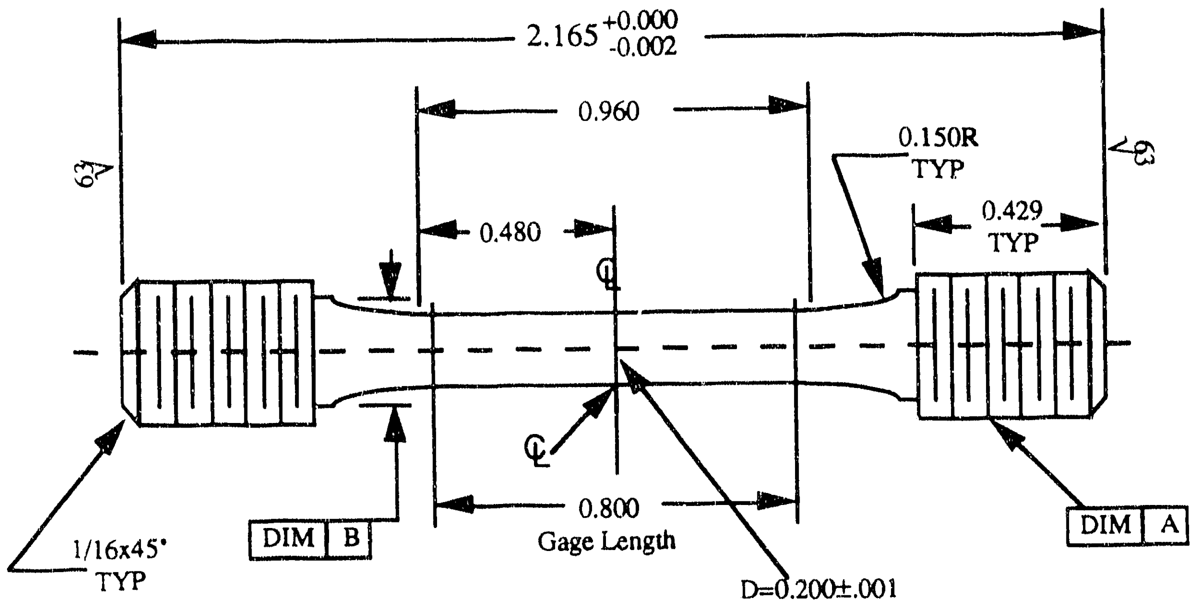

Figure 2: UBR and HFIR Tensile Specimen (Type 2) Dimensions (inches) [11].

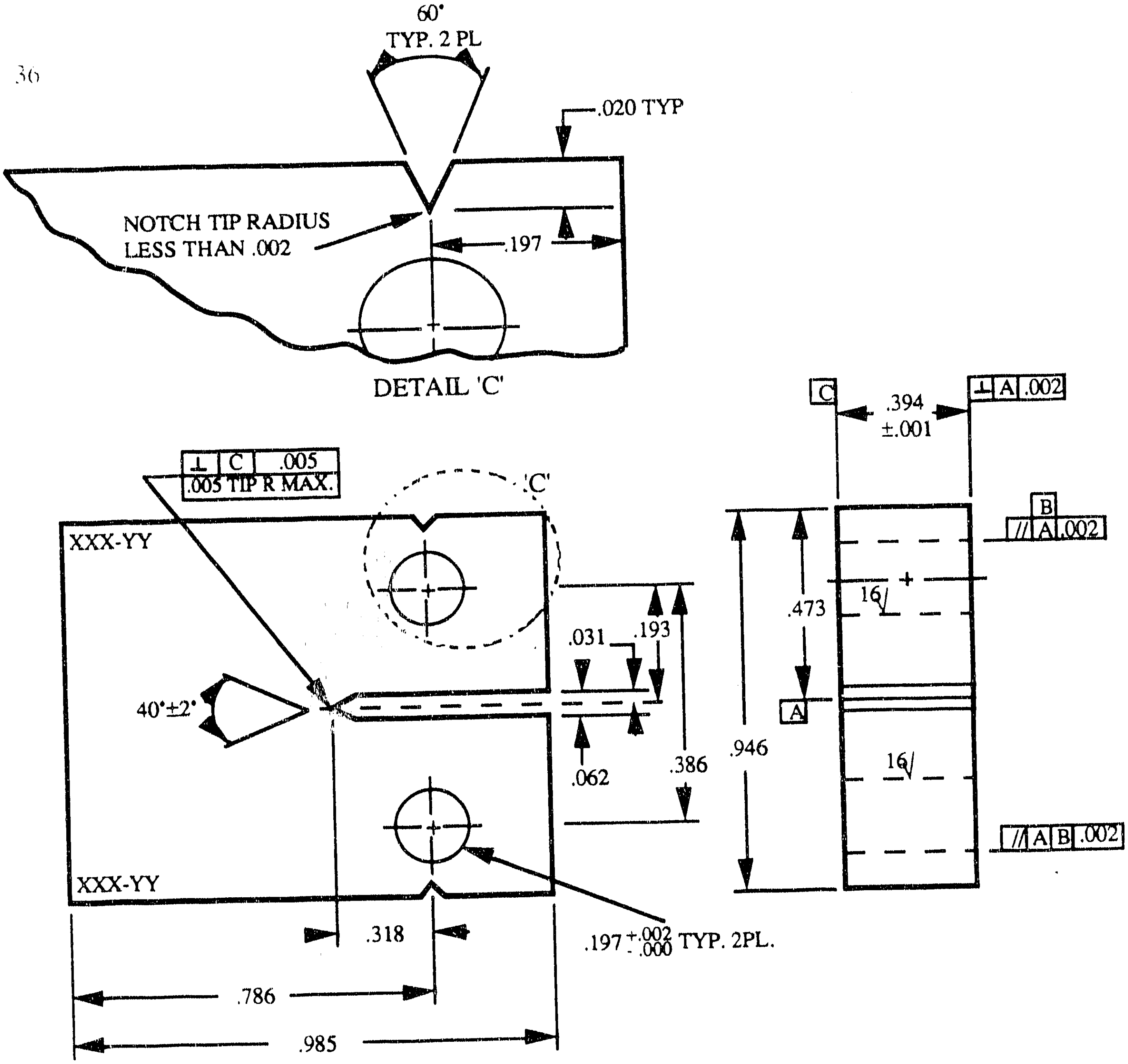

FIGURE 4-4: HFIR 0.4T Compact Tension Specimen Dimensions (inches). The final specimen design included 20% (10% each side) sidegrooving of the notch plane. R-tank CT specimen designs also included this 0.4T design and a 0.8T planform design [11].

Figure 3: CT Specimen Design E399 SR [11].

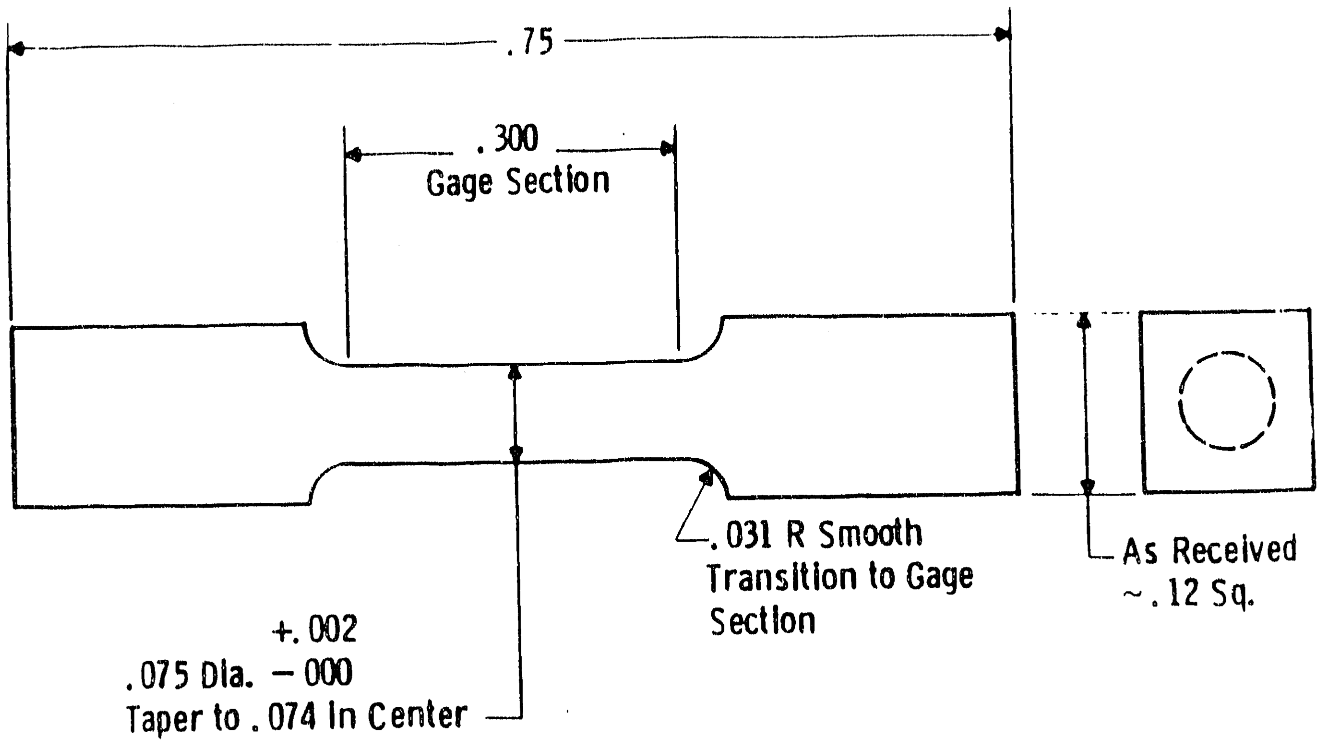

Figure 4: Subsize T Design for R-Tank Materials Testing (inches) [5].

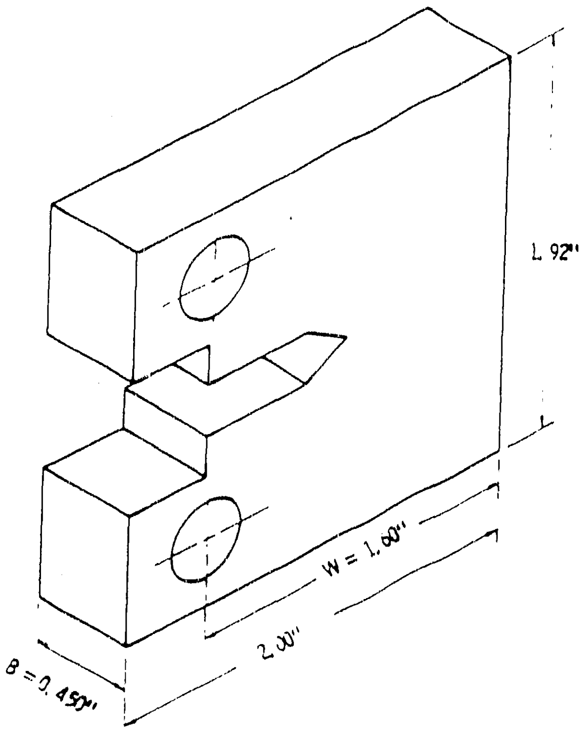

Figure 5: 0.8T-CT Specimen Dimensions (inches). The specimens were not sidegrooved [4].

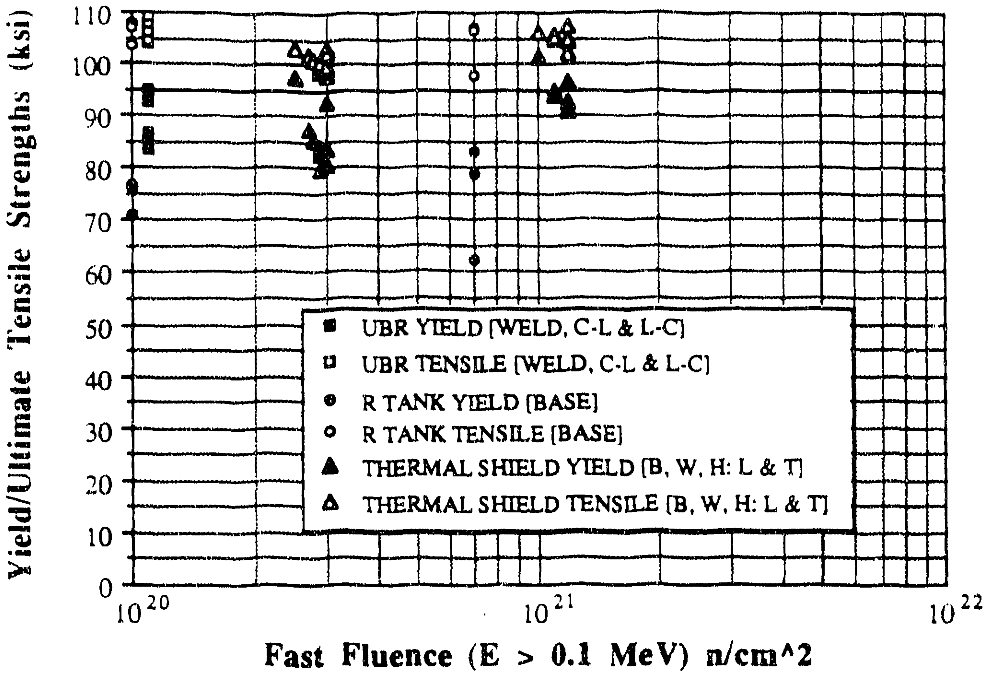

Figure 6A: Yield and Tensile Strengths at 25°C as a function of Fast Fluence ($E_n > 0.1$ MeV) for the UBR, R-Tank, and Thermal Shield Specimens [2].

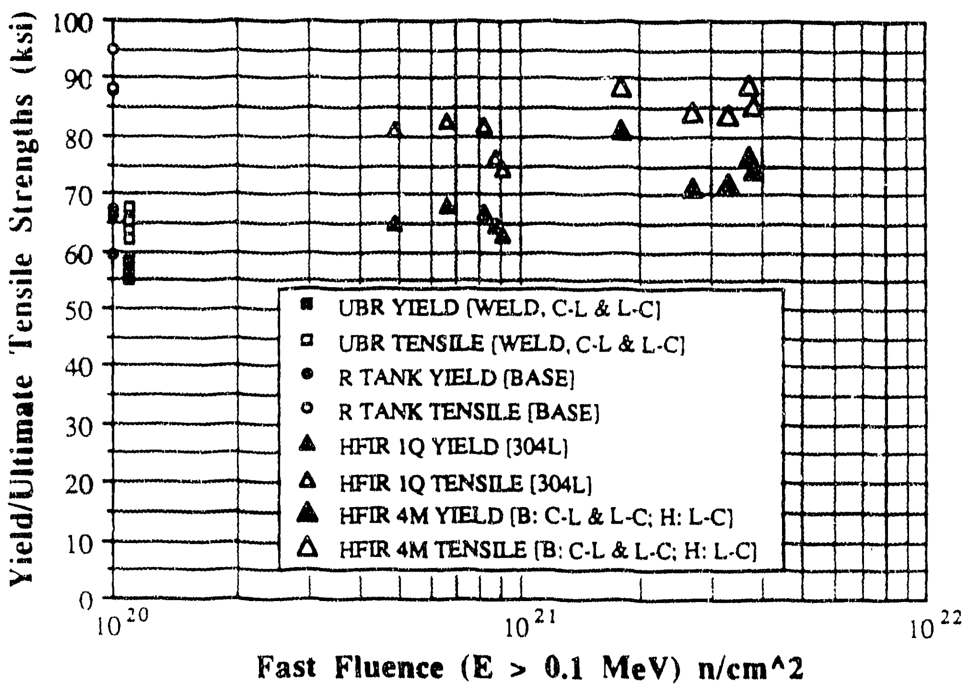

Figure 6B: Yield and Tensile Strengths at 125°C as a function of Fast Fluence ($E_n > 0.1$ MeV) for the UBR, R-Tank, and HFIR 1Q & 4M Specimens [2].

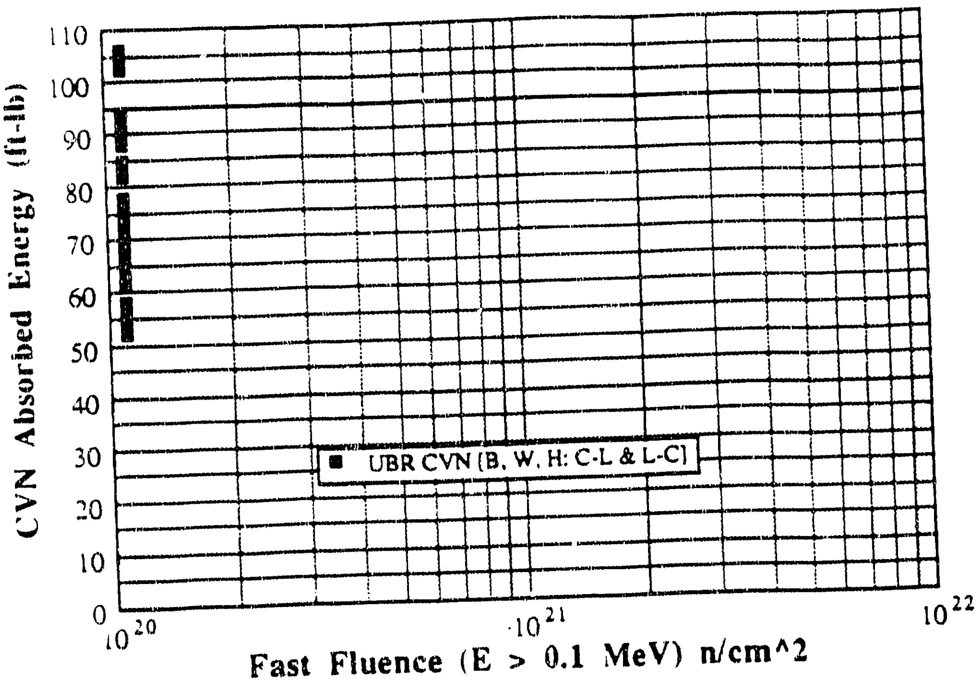

Figure 7A: Absorbed Impact Energy at 25°C as a function of Fast Fluence (E_n > 0.1 MeV) for the UBR Specimens [2].

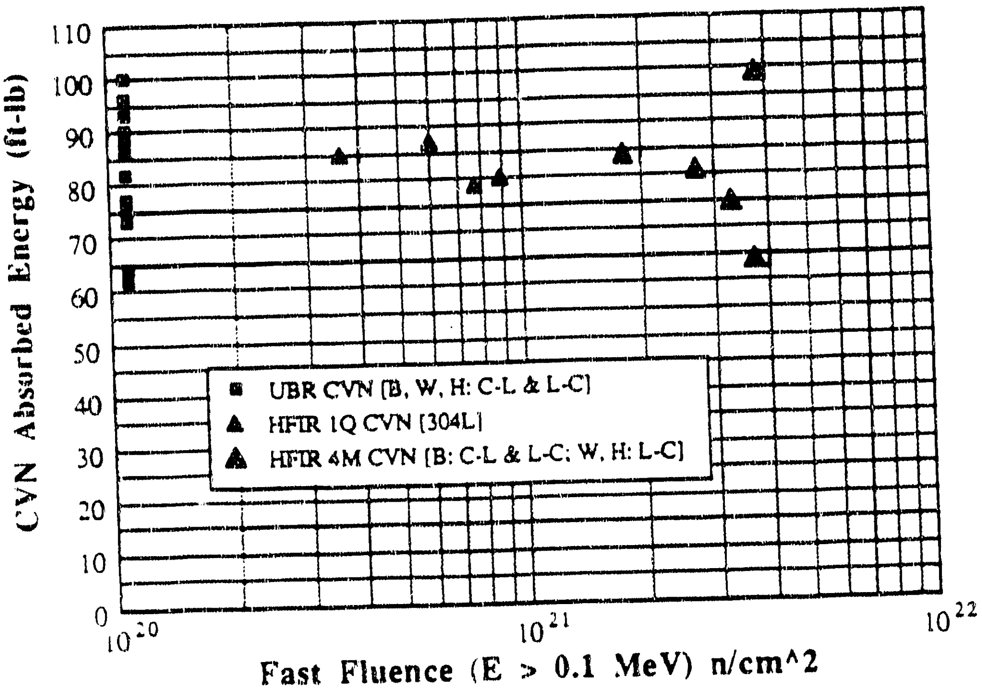

Figure 7B: Absorbed Impact Energy at 125°C as a function of Fast Fluence (E_n > 0.1 MeV) for the UBR and HFIR 1Q & 4M Specimens [2].

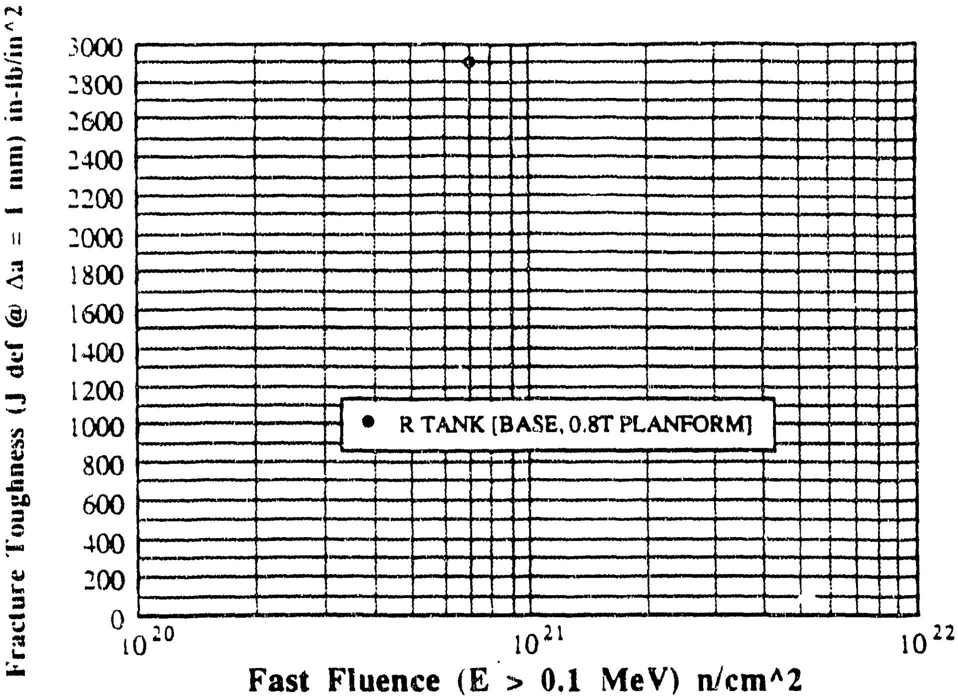

Figure 8A: Fracture Toughness at 25°C as a function of Fast Fluence ($E_n > 0.1$ MeV) for the R-Tank Specimens [2].

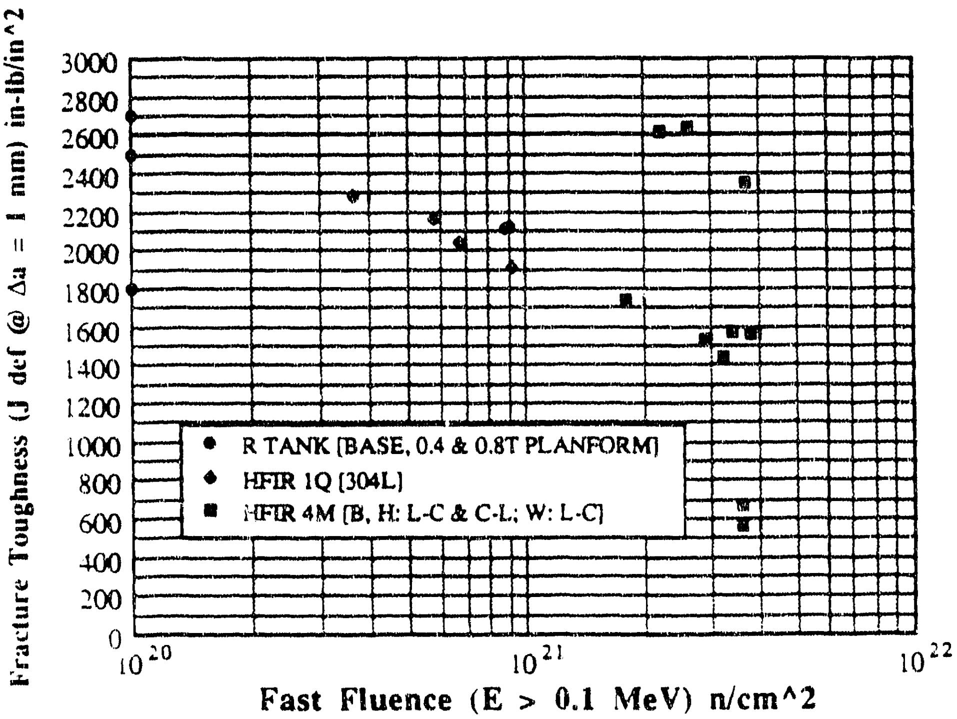

Figure 8B: Fracture Toughness at 125°C as a function of Fast Fluence ($E_n > 0.1$ MeV) for the R-Tank and HFIR 1Q & 4M Specimens [2].

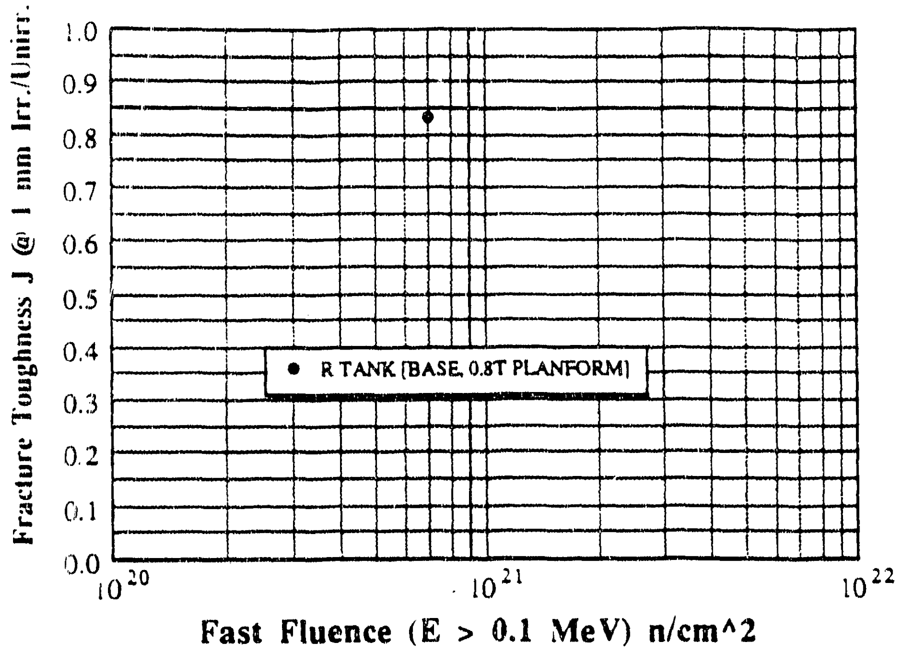

Figure 9A: Normalized (Irr./Unirr.) Fracture Toughness at 25°C as a function of Fast Fluence (E_n > 0.1 MeV) for the R-Tank Specimens [2]. The unirradiated fracture toughness is taken as the average of the L-C and C-L results from the 25°C Base material properties [9].

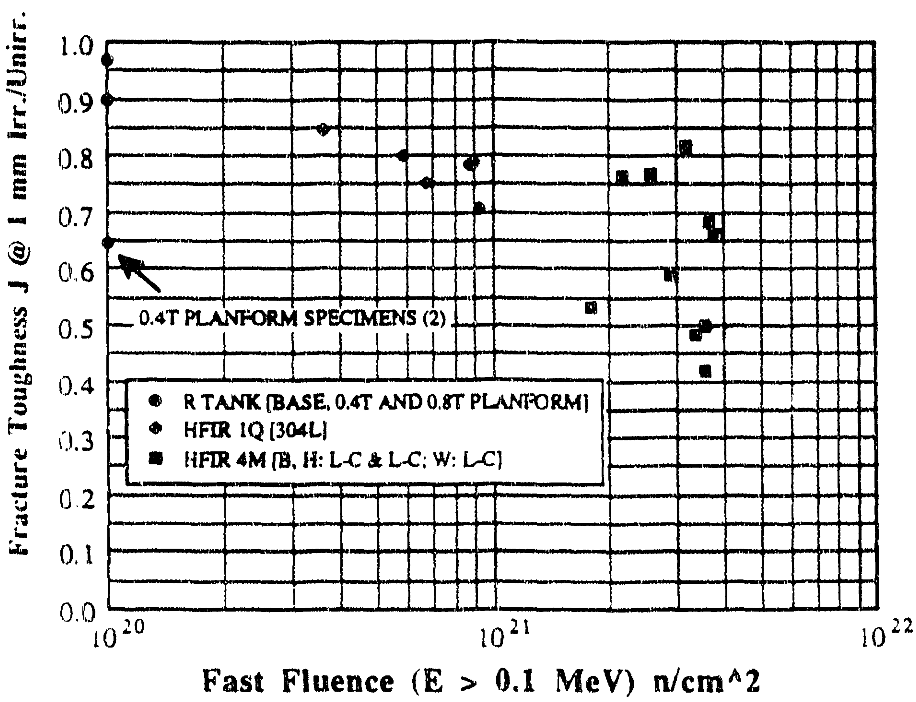

Figure 9B: Normalized (Irr./Unirr.) Fracture Toughness at 125°C as a function of Fast Fluence (E_n > 0.1 MeV) for the HFIR 1Q&4M and R-Tank Specimens [2]. The unirradiated fracture toughness is taken as the average of the L-C and C-L results from the 125°C Base material properties for the R-Tank Specimens [9].

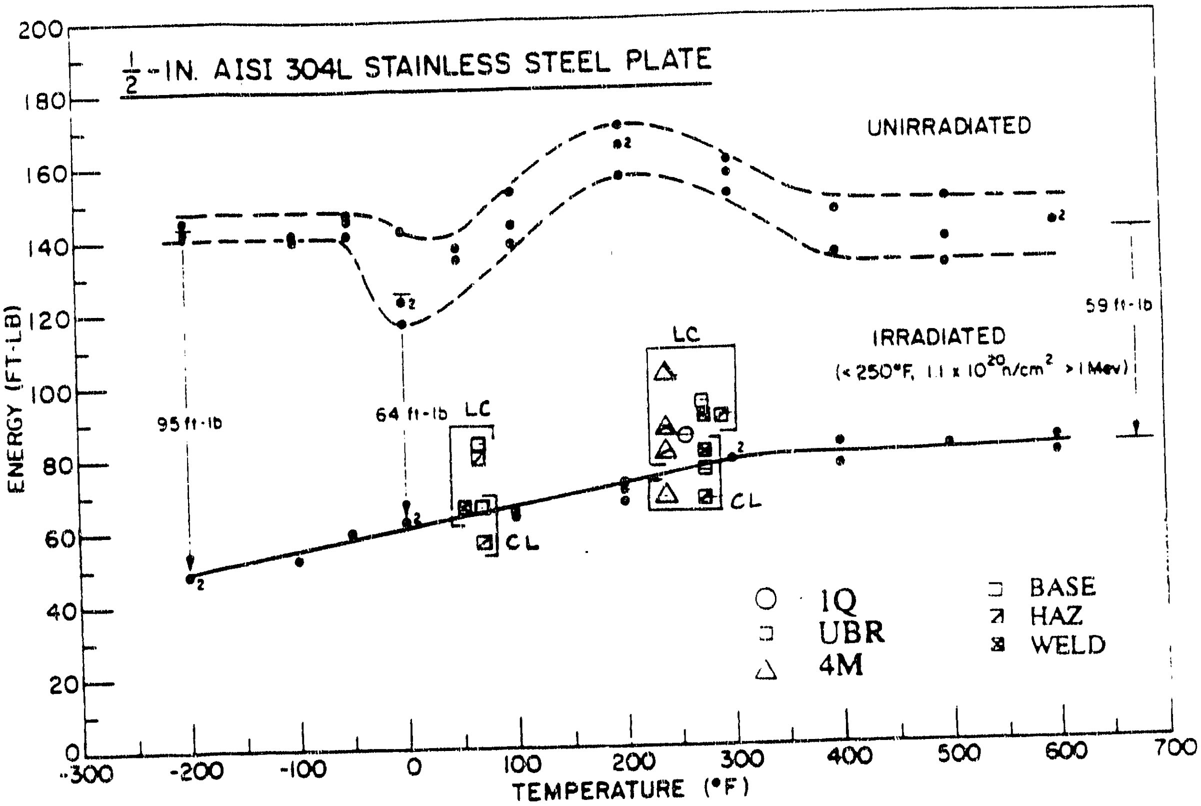

Figure 10: Effect of test temperature on impact energies of irradiated CVN specimens [2, 17].

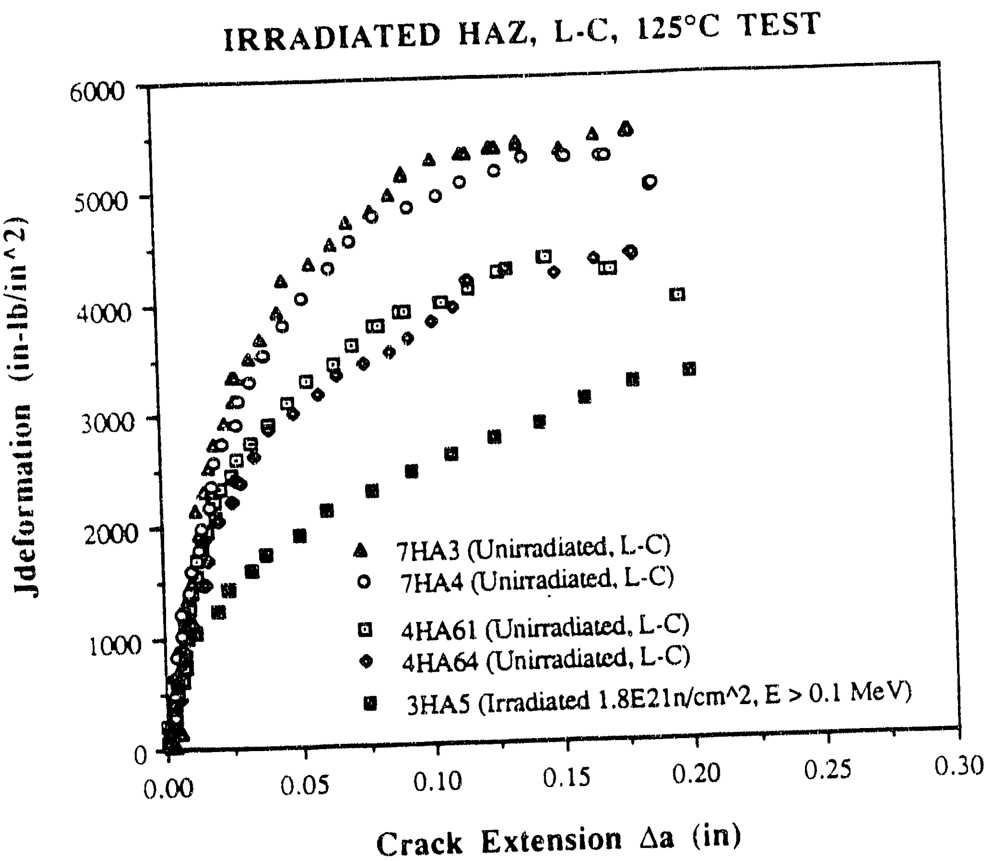

Figure 11: Irradiated vs. Unirradiated J-R Curves for 3HA5 (HAZ/L-C/125°C) [2].

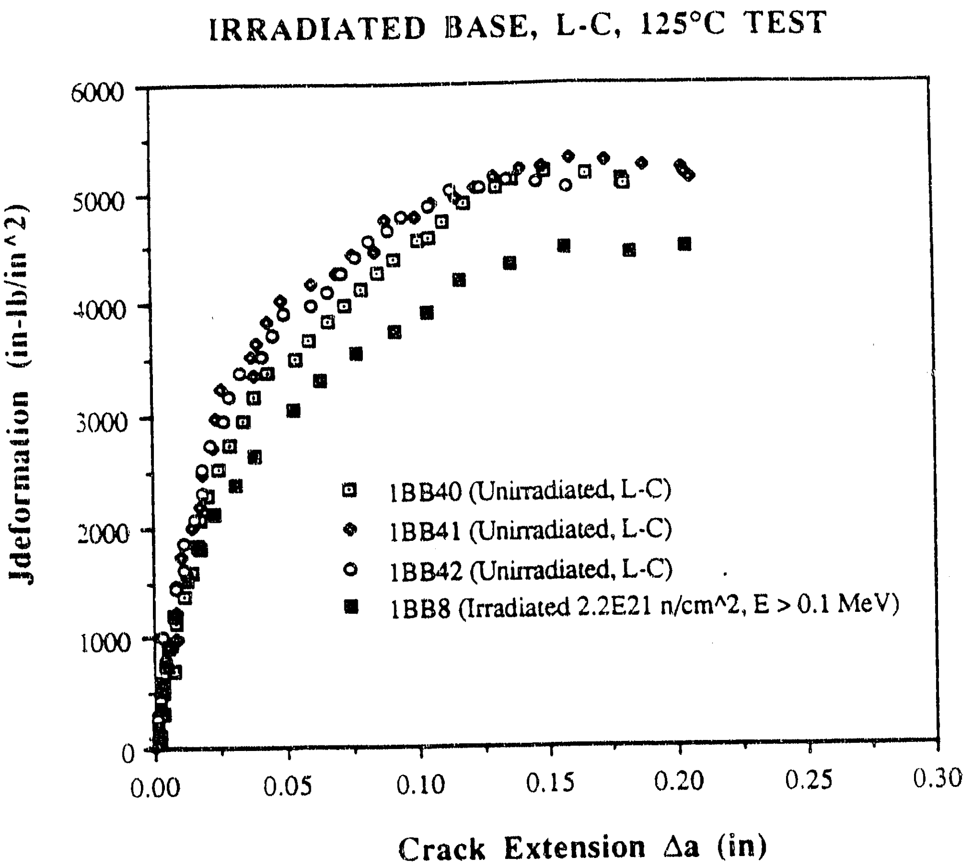

Figure 12: Irradiated vs. Unirradiated J-R Curves for 1BB8 (Base/L-C/125°C) [2].

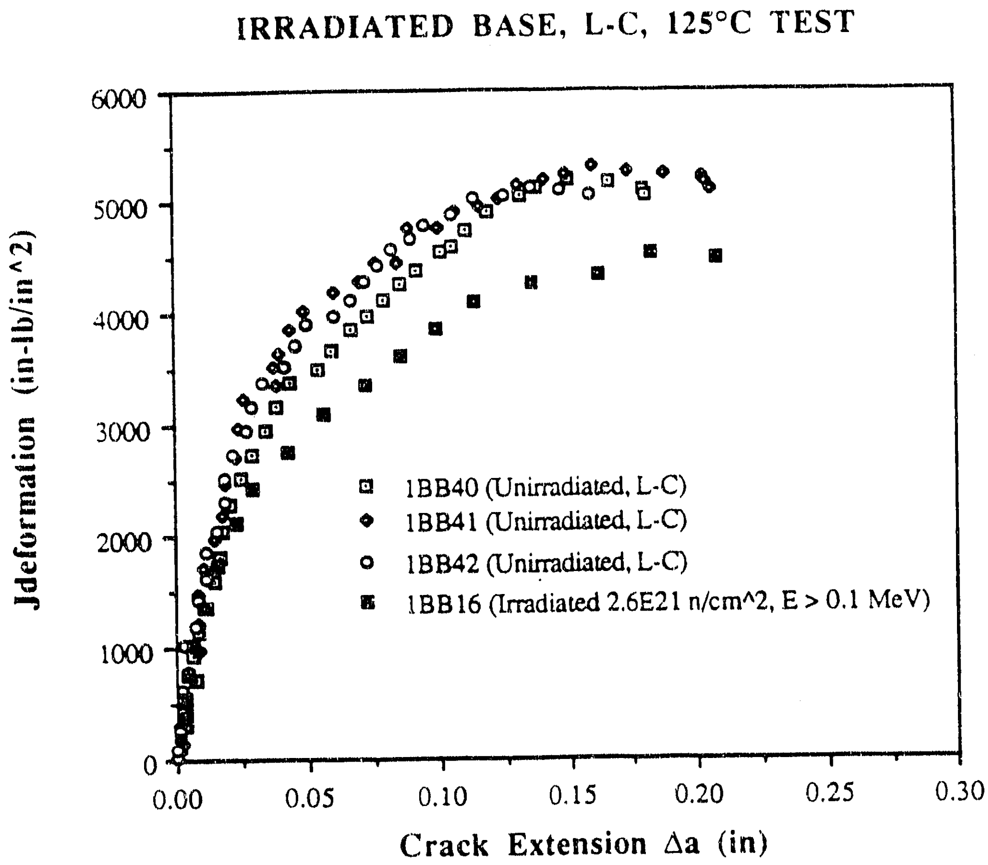

Figure 13: Irradiated vs. Unirradiated J-R Curves for 1BB16 (Base/L-C/125°C) [2].

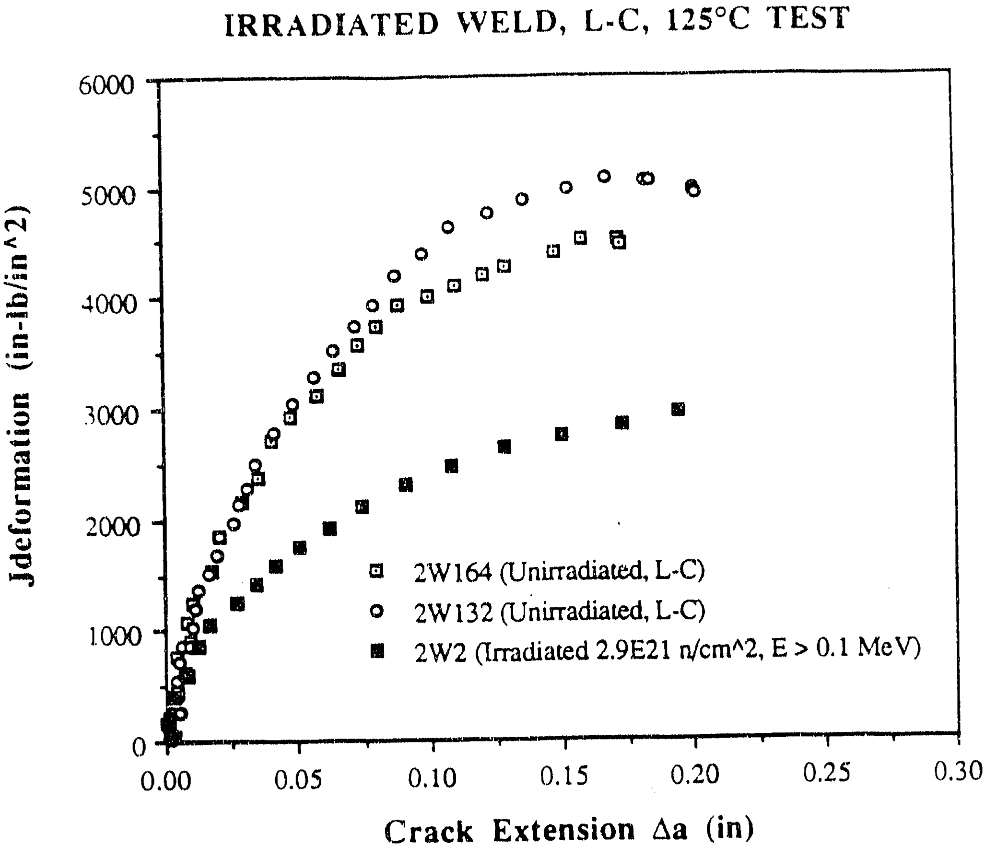

Figure 14: Irradiated vs. Unirradiated J-R Curves for 2W2 (Weld/L-C/125°C) [2].

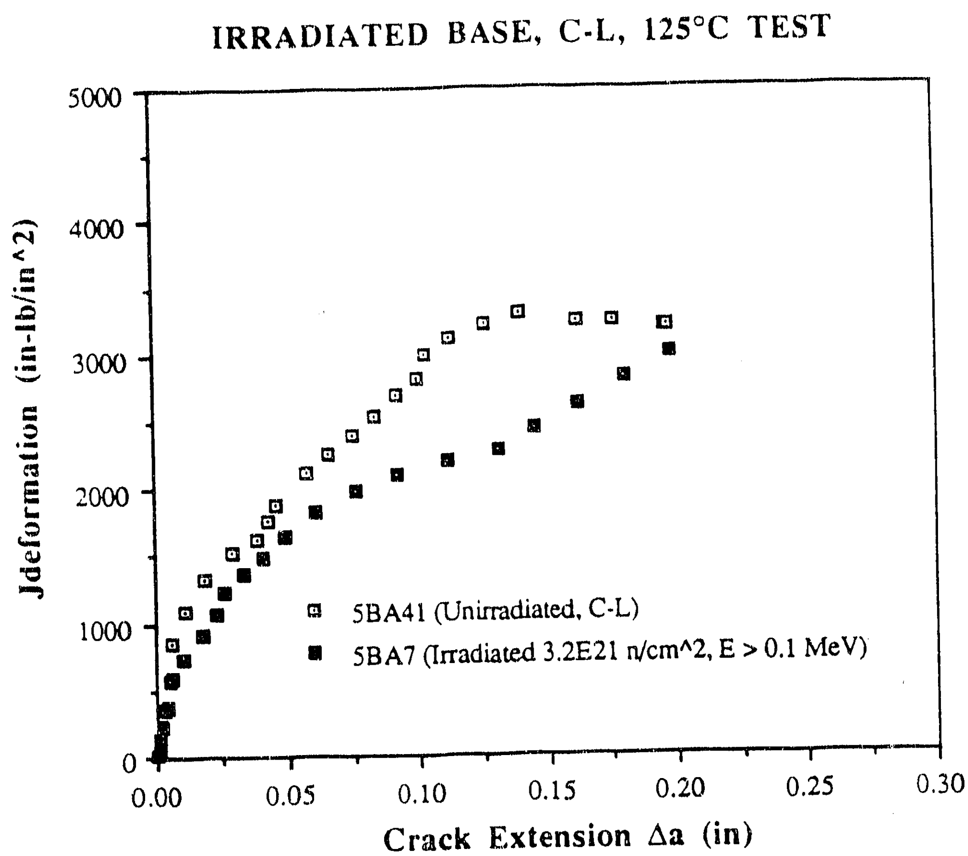

Figure 15: Irradiated vs. Unirradiated J-R Curves for 5BA7 (Base/L-C/125°C) [2].

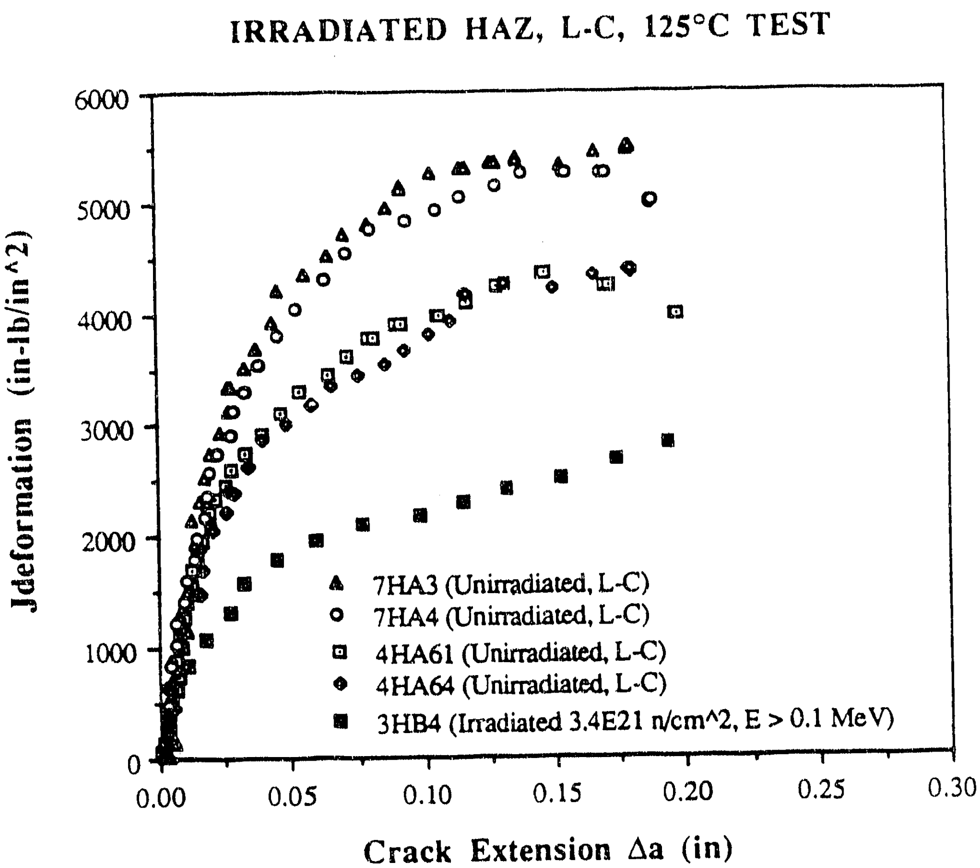

Figure 16: Irradiated vs. Unirradiated J-R Curves for 3HB4 (HAZ/L-C/125°C) [2].

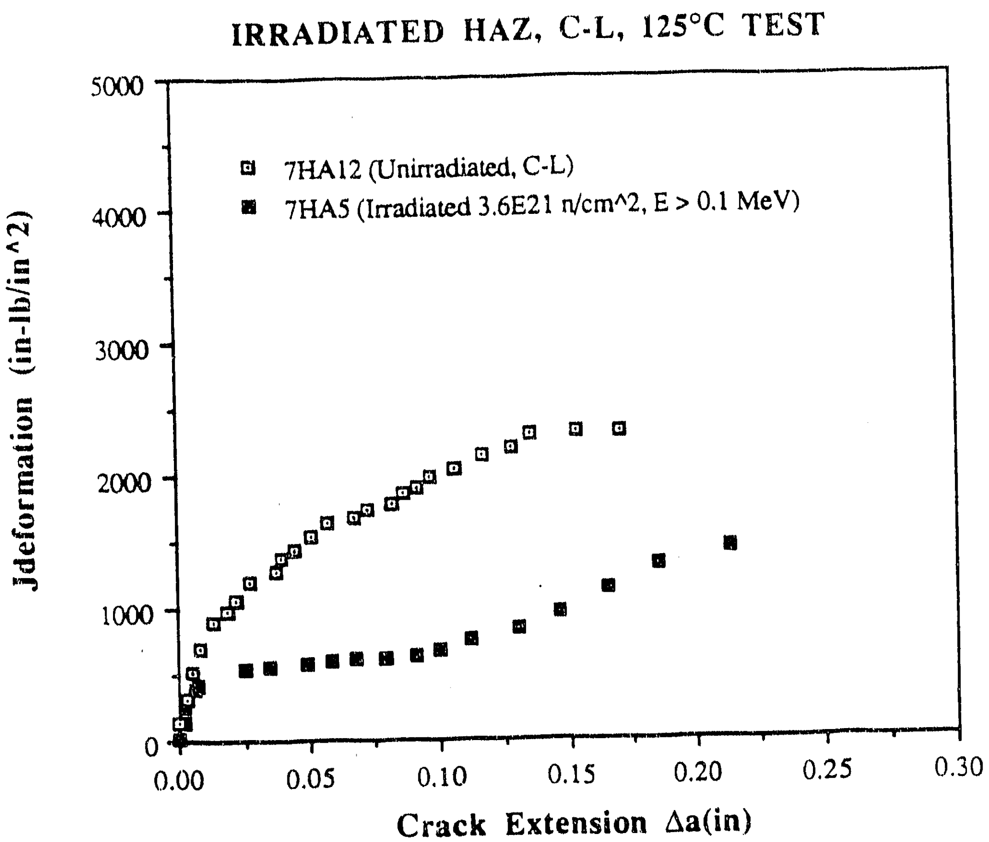

Figure 17: Irradiated vs. Unirradiated J-R Curves for 7HA5 (HAZ/C-L/125°C) [2].

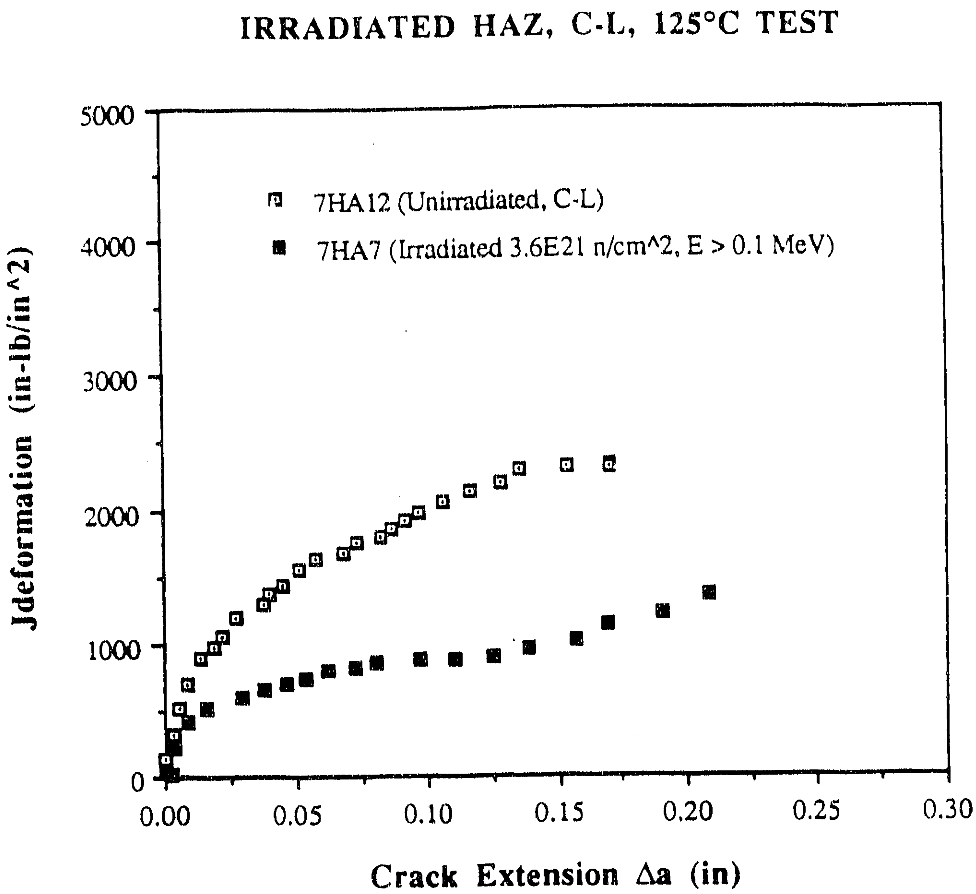

Figure 18: Irradiated vs. Unirradiated J-R Curves for 7HA7 (HAZ/C-L/125°C) [2].

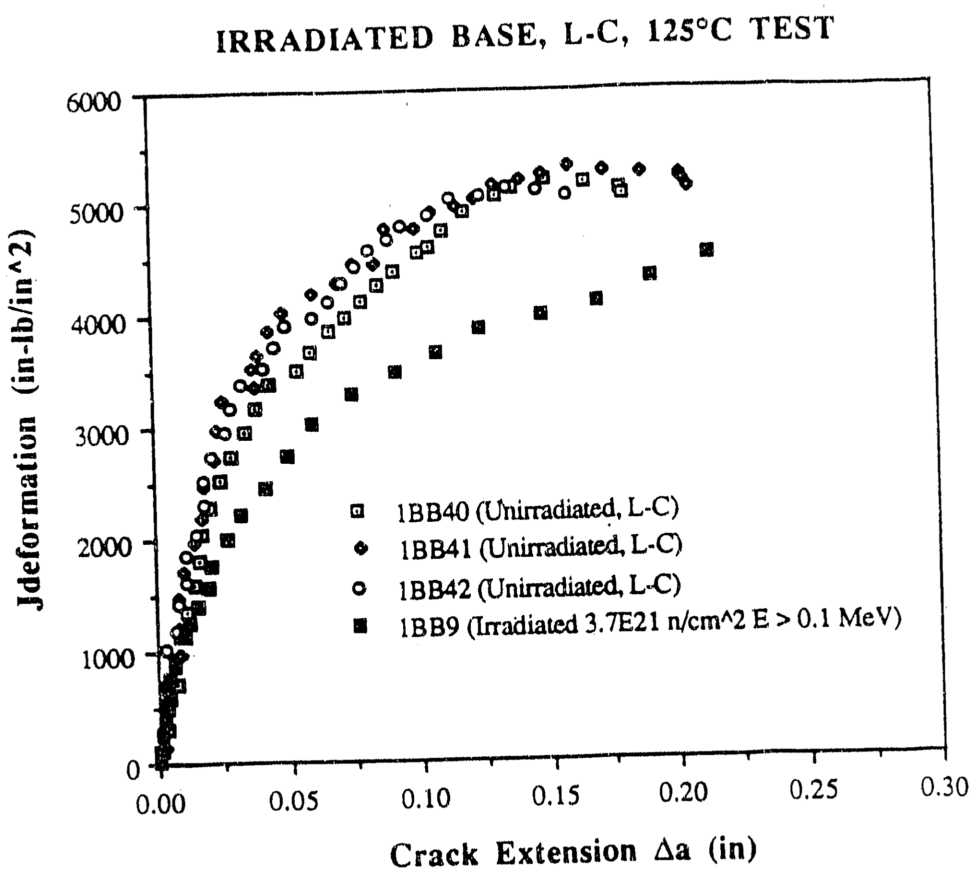

Figure 19: Irradiated vs. Unirradiated J-R Curves for 1BB9 (Base/L-C/125°C) [2].

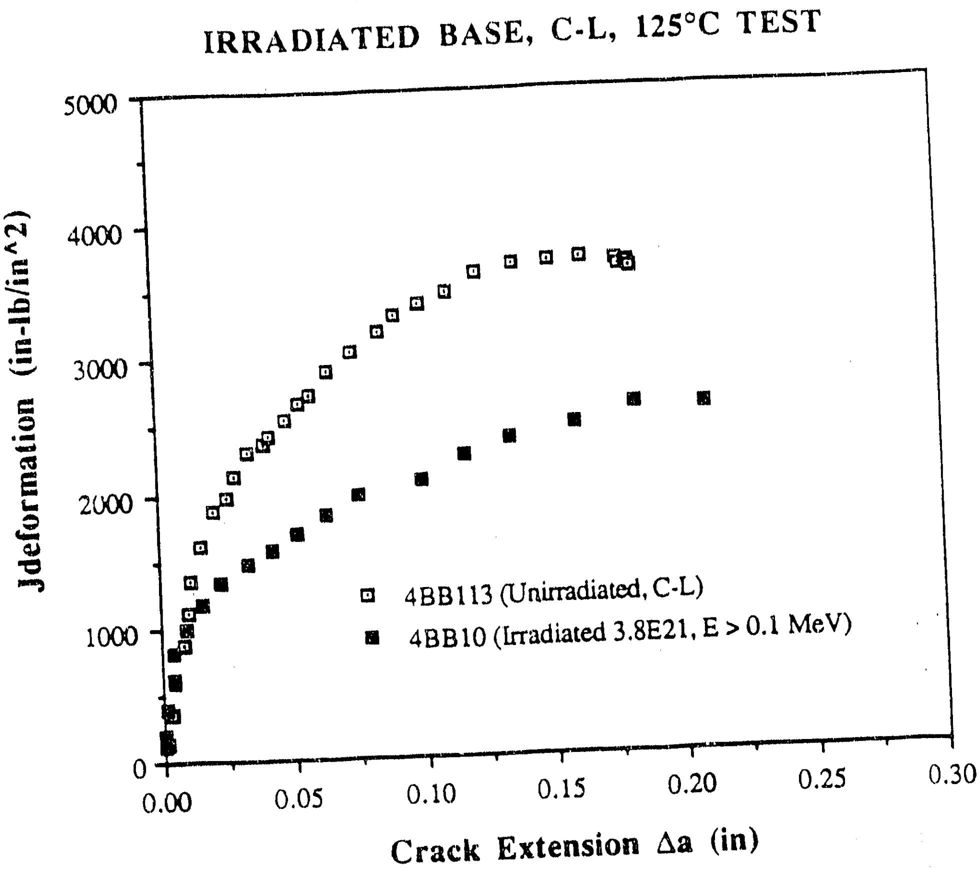

Figure 20: Irradiated vs. Unirradiated J-R Curves for 4BB10 (Base/C-L/125°C) [2].

END

DATE
FILMED
9/4/92